GRAVITY SURVEY OF
SHIRA YOUNGER GRANITE- RING COMPLEX
OF NORTHERN NIGERIA.

BY

ONYIBA NNACHI OGBUOJI
B.Sc. (U.I.) P.G.D.E, (A.B.U.)

Thesis submitted to the Ahmadu Bello University Zaria in partial fulfilment of the requirements for the award of the degree of

MASTER OF SCIENCE IN
APPLIED GEOPHYSICS.

Department Physics
Ahmadu Bello University,
Zaria - Nigeria.

September, 1981

DEDICATION

TO

My beloved, Lord Jesus Christ:

prime sources of Love and Life;

My parents, Ogbu and Mary:

prime sources of motivation;

My wife, Maureen; children, Chimdinma, Rapture, Ebenezer and Elias:

prime sources of support and encouragement.

DECLARATION

This thesis is an original work carried out by the author under the supervision of Professor D.E. Ajakaiye. To the best of my knowledge no part thereof has been submitted elsewhere for the Award of a degree or diploma, and the work of others is acknowledged and referenced.

Prof. D.E. Ajakaiye
(Supervisor).

C. N. OGBUOJI
(Author).

AHMADU BELLO UNIVERSITY
Z A R I A.

SEPTEMBER, 1981.

CONTENTS

Page

Page

----oOo----

ACKNOWLEDGEMENT

I wish to thank Professor D.E. Ajakaiye, Head of Department of Physics, for accepting the topic and to acknowledge her excellent supervision both in the design and execution of the project.

Also I wish to express my profound gratitude to all the members of the geophysics team. I am grateful to the course co-ordinator, Mr. S.E. Ananaba for his constant advice throughout the duration of the project and during the entire course. To Mr. M.N. Umego I am greatly indebted for his personal concern to see me through the course and for his help in reading through my drafts. To Mr. I.B. Osazuwa I am grateful for his concern and help in giving me useful materials for the project.

I am indeed very grateful to Dr Awad for his friendly and continuous guidance in the interpretation of the data.

I will like to thank Mr. P.J.T. Verheijen for checking through my computations.

My thanks goes to Mr. K.K. Ibe, a geologist, who accompanied me to the field to identify some samples. I am also grateful to Dr. E.C. Ike of Geology Department for reading through the geology chapter and for identification of the samples.

I am greatly indebted to Mr. G.I. Nwafor of the Geological Surveys, Kano for providing me with transport when I needed it.

Finally to all and sundary who contributed in one way or the other to make the course a success, I am greatly indebted.

LIST OF FIGURES

ABSTRACT

The gravity survey over the Shira Younger Granite Ring Complex is aimed at investigating the subsurface structure of the ring complex whose three main rock types are arfvedsonite granite, biotite granite and syenite.

Density determinations of the rock samples in the area gave values of 2.62 x 10^3 kg m^3 for arfvedsonite granite, 2.58 x 10 kg m^{-3} for biotite granite- and 2.66 x 10^3 kg m^{-3} for syenite.

A pear-shaped positive Bouguer anomaly striking S W was observed over the arfvedsonite granite and biotite granite which forms the northern part of the complex. While at the southern section, over the syenite, the Bouguer anomaly is predominantly negative with an E - W trend. The residual gravity anomalies of the northern and the southern sections are of amplitudes + 70 g.u. and - 80 g.u. respectively. These suggest that the northern section of the complex had been intruded at depth by a high density material possibly basalt, possibly after the formation of the complex.

The subsurface structure of the Shira Younger Granite Ring Complex consists of three layers at depth. The rock type that is least exposed arfvedsonite granite is the most deeply seated, while the highly exposed, most dense-, syenitic massifs is the least in subsurface thickness and is else the uppermost layer.

One of the profiles interpreted indicate that the syenitic massif extends from the ground surface to a depth of 1.0 km. This is underlain by the biotite granite mass whose thickness is 2.0 km. which is in turn underlain by the arfvedsonite granite body located at a depth of 2.5 km. to 4.0 km.

CHAPTER ONE

INTRODUCTION

1.1 The Present Work:

The work presented in this thesis is a survey of the Shira Younger Granite Ring Complex which lies between latitudes 11° 40.60' N to 11° 19.24' N and longitude 10° 11.72' E to 09° 55.17' E. Shira town in Bauchi State of Nigeria lies within the complex (fig. 1). The Chad Basin lies along the northern and north-eastern frontier and no other ring complex in known to exist beyond this Shira complex. The Shira complex is bounded in the south by the Kila-warji, Dogo Dutse and Fagam Younger Granite Ring Complexes (fig. 2).

The gravity data was colleoted along most roads and tracks that run through the complex. A total of 127 km was surveyed (fig. 3).

The relief in the area is generally low (about 400 metres above sea level) except within the complex where its elevation is as high as 480 metres. Along traverses within the complex a maximum height - difference of about 80 metres were encountered but

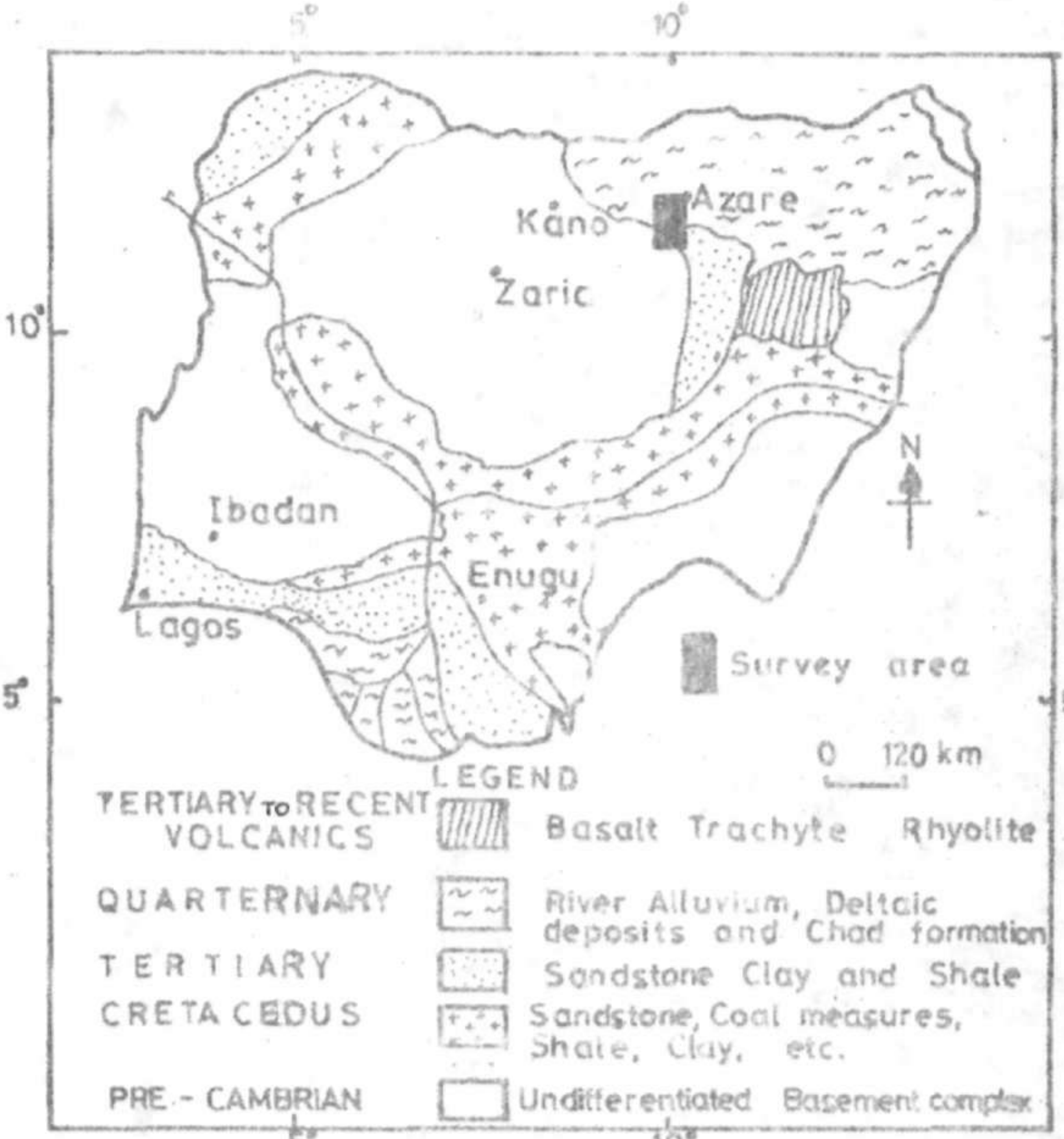

Fig.1 Simplified Geological Map of Nigeria

outside the complex the height differences were less than 20 metres.

1.2 Previous Geophysical Work on the Nigerian Younger Granite Province:

Early geophysical work done on the Nigerian Younger Granite Province was prompted by economic need because of its mineralization. On the Jos Plateau, resistivity and magnetic surveys were carried out to locate buried channels where alluvial tin were suspected to be buried (Du Preez, 1948; Shaw, 1950; Shaw and Cole, 1961). In 1963, an Aero-magnetic map was published by the Canadian Aero-Service Limited. This was followed by a ground survey consisting of magnetics, seismics, resistivity and gravity (Masson-Smith, 1965).

Other research work in the area not prompted by economic considerations include a regional gravity survey of some parts of the province (Cratchley and Jones, 1965) and a regional gravity survey of the province (Ajakaiye, 1970).

Some of the ring complexes in the province have been surveyed in detail. These include Ririwai (Liruei) Younger Granite ring complex (Ajakaiye, 1968); the

Banke Ring Complex (Ajakaiye 1974); the Dutsen-Wai complex (Ajakaiye and Sweeney, 1974) and Dutse complex (Amosu, 1980).

1.3 Choice of Geophysical Method:

Geophysical instruments are nothing more than auxiliary eyes temporarily substituted for our conventional method of observation of the Earth (Hanson, 1966).

Acid intrusion such as the Younger Granites are almost invariably associated with negative Bouguer anomalies (Bott, 1955). These anomalies are caused by direct density contrast between the less dense granite intrusion and the denser country rock forming the basement.

Several large negative anomalies which cannot be attributed to any exposed structure, seem only reasonably interpreted as due to unexposed granites (Goguel, 1950; Bott, 1954).

The results of previous geophysical surveys of other Younger granite complexes do show that the gravity method has been very effective in delineating both exposed and buried complexes. Even very close complexes have been clearly resolved on the basis of gravity results (Bott, 1955; Ajakaiye, 1968, 1974; Bott and Smithson, 1967).

The Shira complex has been geologically identified as a Younger Granite ring complex (Turner, 1976). Hence the choice of the gravity method for this survey is logical and consistent with earlier results of other geophysical work on the Younger Granite Province of Nigeria.

CHAPTER TWO

GEOLOGY

2.1 The Granite Problem:

The granite problem can be studied from the point of view of their surface features and emplacement of granitic bodies.

A granitic rock is a coarse grained acid igneous rock, consisting essentially of quartz and feldspar with minor proportions of dark minerals such as mica, amphibole or pyroxene and occasionally fayalite. They are massive in structure but within a single mass there may be variations (Turner, 1968).

Daly (1933) has shown that granites form 95 per cent of all plutonic intrusions. The plutonic associations included systectonic, posttectonic and atectonic granites.

Falconer (1911) divided the granitic rocks in Nigeria into two types, namely the Older and Younger Granites. The Younger Granites cut across all structures in the basement including those of the older granites. They give rise to rugged, well exposed massifs. The Older Granites on the other hand tend to conform with the structure of gneisses and migmatites of the basement complex, but show a more subdued relief.

The two schools of thought on the origin of granites are the magmatic and the metasomatic views. Based on the magmatic hypothesis there are two possible main mechanisms for emplacements. These are: that there was a forcible intrusion as a result of external or internal forces or that there was a permissive intrusion during the aneorogenic episode (Bowden, 1970). The metasomatic hypothesis implies the sediments and metamorphic rocks are converted to granite by metasomatic changes (Bowden, 1970).

2.2 The Nigerian Younger Granite Province:

The Nigerian Younger Granite Province shown in fig 2 comprises over forty individual ring complexes of Triassic to Jurassic age (Van Breeman and Bowden, 1973).

Location of ring complexes are not random. They are confined within a distinct region and show clustering and alignments which suggest that pre-existing structures may have controlled their location. Lines of weakness in the basement appear to have influenced the location. The clearest example of basement control is seen in the

THE NIGERIAN YOUNGER GRANITE RING COMPLEXES

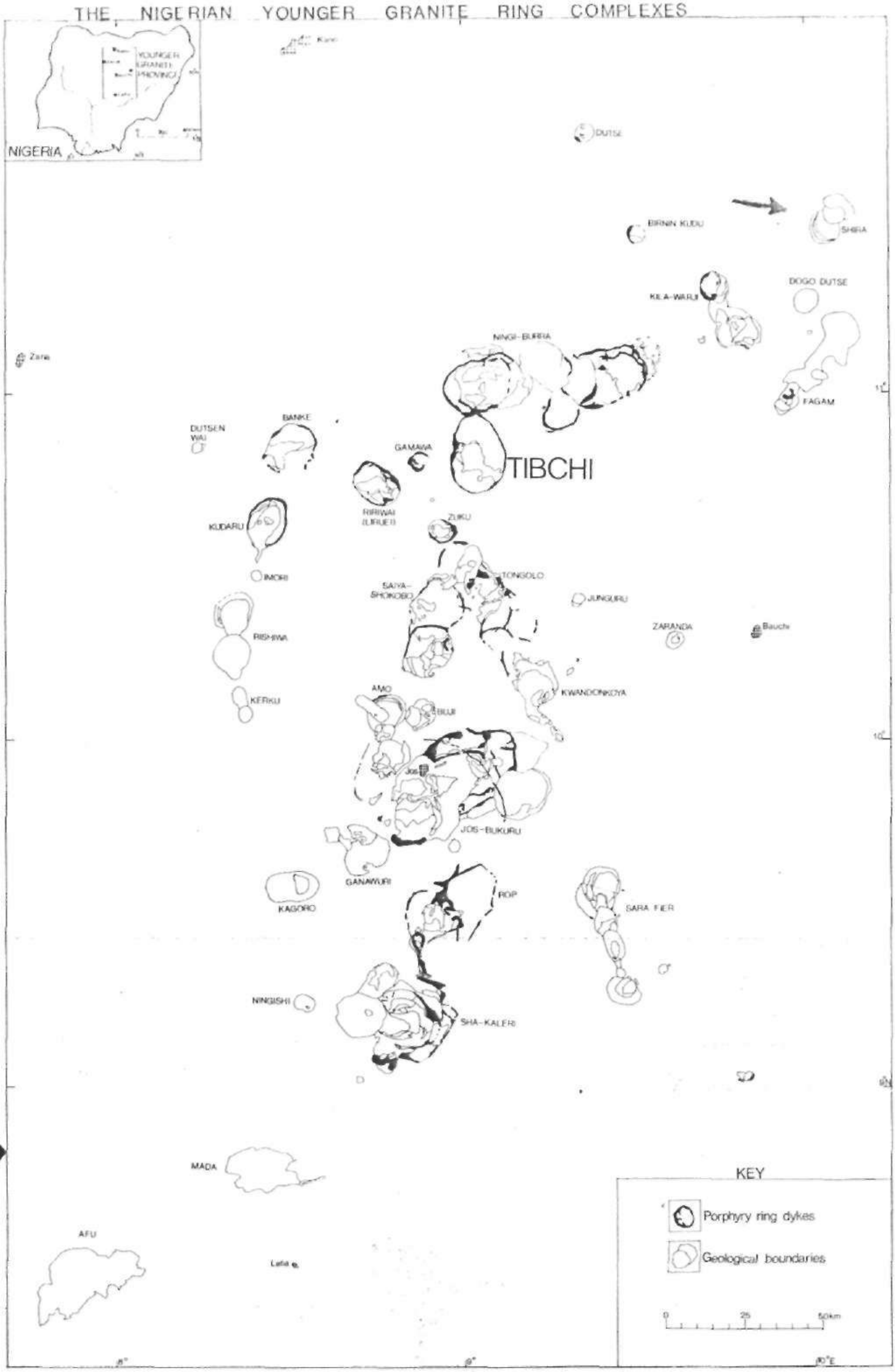

Fig 2

NNW and NNE alignments of the ring complexws, parallel to zones of shearing, which accompanied the emplacement of late instrusions in the older granite series. Other directions of ring complex alignment corresponds to basement joints and fractures (Turner, 1973).

Black (1969) has postulated that the development of the Mesozoic Nigerian Younger Granite province and the disruption of the Gondwanaland may be related to the same cause, namely that the linear distribution of the ring-complexes reflects the former location of a zone of high heat flow in the mantle. Wright (1971) has observed that the province also lies on a continuation of the African continental margin to the south and was possibly formed in a region of a crustal arching developed prior to the separation of African and American plates in the Cretaceous.

The Younger Granites intruded a sediment-covered depression of late Precambrian to early Palaeozoic basement rocks of northern Nigeria in a N - S zone which continues northwards to the arid region of Niger Republic (Black and Girod, 1970).

2.2.1 The Ring Complex Evolution:

The ring complex of Nigerian Younger Granite province development followed a regular pattern of intrusive and extrusive activity which is observed to repeat throughout the province (Turner, 1972, 1973).

Turner (1963, 1972) subdivided the activities into three phases. Phase one is a long and varied early volcanism. This early volcanic activity was brought to a close by the major cauldron-subsidence; the sinking of a cylindrical mass of country rocks and volcanic rocks into the underlying magma-chamber, with the formation of a peripheral ring-dyke of granitic-porphyry.

This was followed by a granitic phase of entirely sub-surface activity. This began with an intrusion of riebeckite-aegirine granite, rising along the ring fracture and invading the rhyolites within the ring-dyke.

The final phase is the emplacement of a succession of granites within this ring-fault, generally in a concentric fashion. Among the granites emplaced is hornblende-biotite, biotite and riebeckite.

The ring-complexes of the Nigerian type constitute a link between surface volcanic features and their deep-seated magmatic sources (Bowden, 1970).

A notable feature of the Younger Granite is that both intrusions and extrusions are almost completely restricted to within the confining ring-fault of each centre, suggesting that the magma-chamber was similarly limited in size.

2.2.2 The Structure, Petrology and Mineralization of the Younger Granites of Nigeria:

The Younger Granites of Nigeria are of varied sizes, many of the larger ones being made up of two or more overlaping ring complexes (fig 2). They occur in a broad N - S zone approximately 60,000 km^2 with the centre on the Jos Plateau where the greatest concentration of ring complexes exist (fig 2).

The ring complexes form distinct structural features in the Younger Granite province because of the high degree of exposure and varying structural depths to which erosion has penetrated (Turner, 1968). The northern ring complexes (including Shira) are exposed at a higher structural level. They are less deeply eroded than those of the Jos Plateau and the southern complexes (Turner, 1973).

According to Turner (1980) the rock types can be divided petrologically into six groups. These are biotite granite; early and late rhyolite; granites and porphyrites; aegirine - arfvedsonite granites; syenite and trachytes; gabbros, diorite, dolerites and basalts, these occupy areas in percentage of 45.1; 18.7; 17.8; 14; 3.8 and 0.6 respectively.

The subvolcanic nature of the granites is shown by the textural sequence from rhyolites originally glassy through porphyries to coarse grained granites. In the northern part of the province there is abundant rhyolite associated with fayalite granite - porphyries and peralkaline granites. In the central and southern parts of the province, the complexes are exposed massifs of biotite and hastingsite biotite granites.

The Younger Granites Province is the major source of Nigeria's minerals such as tin (cassiterite) and columbite. Other mineralization of economic importance in the province are wolfram, molybdenite, monazite, zircon, thorite, genethelvite, fergusonite and pyrochlore. Several minerals have been discovered in Shira complex these include aegirine-hedenbergite, chevkinite and narsarsukite (Bennett, 1981).

2.2.3 The Shira Younger Granite Ring Complex:

Most of the ring complexes have been mapped geologically (Bain, 1934; Jacobson, 1947; Bowden and Turner, 1974; Ike, 1979; Bennett, 1981), field investigations suggest that the Shira complex is dominated by peralkaline syenites and granites which occupies an area of about 152 km^2 (Bennett, 1981).

This complex can be divided into three sections S_1, S_2 and S_3. S_1 is dominated by the Shira quartz syenite and this has been intruded by a large cone sheet of aegirine arfvedsonite granite and by microgranite dykes (fig 3). These peralkaline syenites and granites are believed to represent successive intrusions from a progressively differentiating magma chamber. The aegirine arfvedsonite granite has two facies distinguished by the habit of the arfvedsonite and both facies exhibit layering. S_2 is composed of the ferrorichterite-arfvedsonite granite and a small intrusion of syenite (fig 3). S_3 consists of the very poorly exposed aluminous biotite granite.

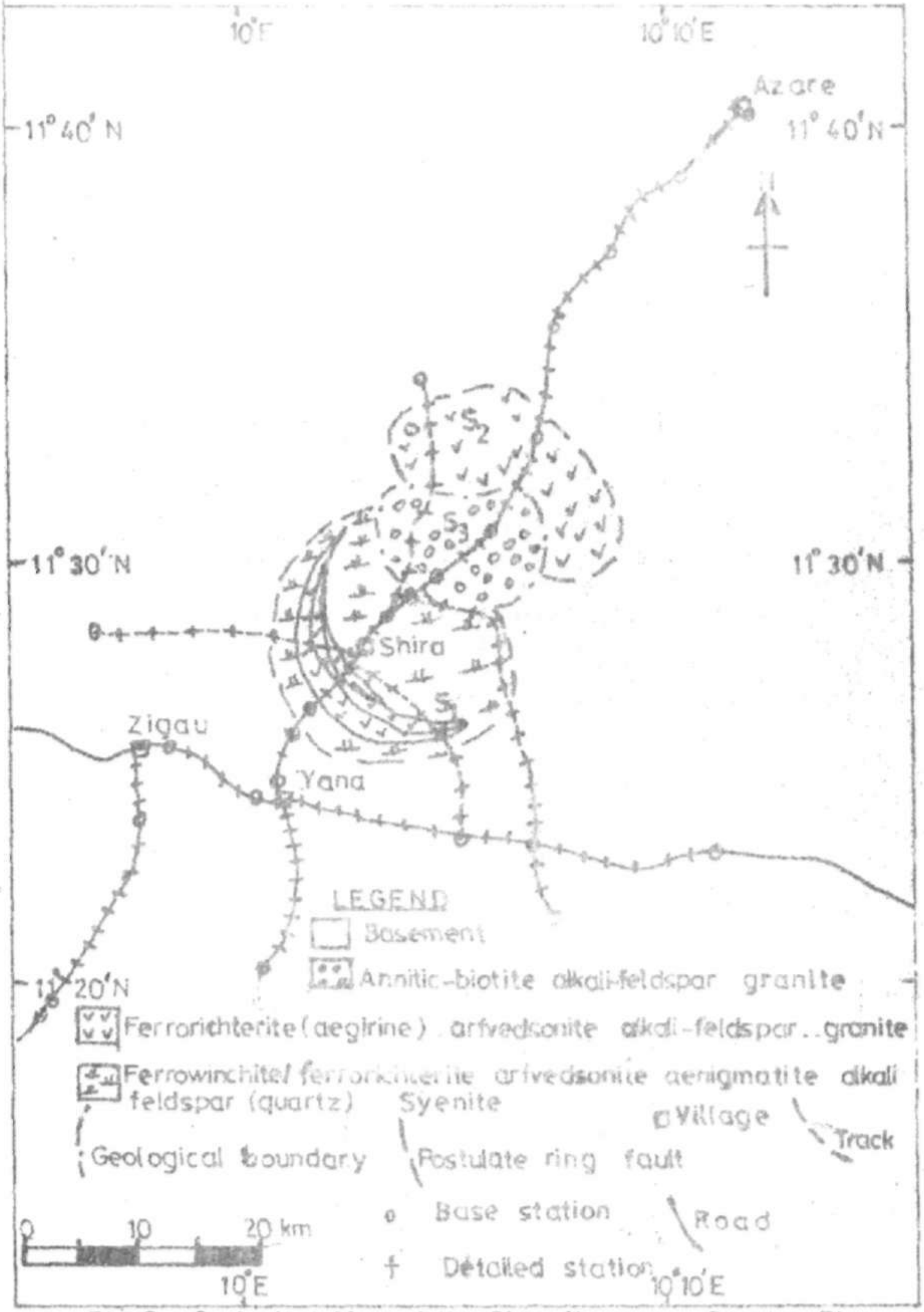

Fig-3 Geological Map of the Shira Younger Granite Ring Complex (After Bennet, 1981) Showing Gravity stations.

The Shira quartz syenite consists of microperthite, quartz, ferrorichterite - arfvedsonite and a little aegirine, and the dykes related to it have a similar mineralogy but are more mafic-rich. The granite (S_2) consists of microperthite quartz, ferrorichterite-arfvedsonite and aegirine. The small syenite intrusion on S_2, has three facies which collectively contain microperthite quartz, ferrowinchite-arfvedsonite, aenigmatite and aegrine. The granite (S_3) contains microperthite, quartz and biotite.

Whole rock geochemical data suggest that there is a progression from the syenites to the highly fractionated granites. With regard to the accurence and characteristics of the peralkaline and aluminous granites in particular, it is concluded that the peralkaline syenites and granites from Shira are the result of fractional crystallization from a basaltic parent, whereas the aluminous rocks are the result of partial melting in the continental crust (Bennett, 1981).

CHAPTER THREE

FIELD PROCEDURES AND INSTRUMENTATION

3.1 Field Procedures:

The vertical variations in density of horizontal layers affect all observations to the same degree (Hinze, 1966). These variations therefore will not cause any observed anomaly at the stations. The horizontal variations in density of the crustal layer will cause variations in the observed gravity readings.

Fortunately the Younger Granite Province has been associated with a Bouguer negative gravity anomaly (Ajakaiye, 1970). Younger Granite intrusive have comparatively lower densities of about 2.66 x 10^3 kg m^{-3} than the surrounding basement rocks of density 2.67 x 10^3 kg m^{-3} thus resulting in a density contrast of about 0.01 x 10^3 kg m^{-3}. Hence the choice of the gravity method in this study of the Shira Younger Granite Ring complex is consistent with earlier methodology.

The gravity survey was carried out along the traverses indicated in figure 3 between January and May, 1981. The traverses consists of a major road and tracks running through the complex and other roads in the vicinity of the complex.

There were 23 base stations established in the survey (fig 3) and detail stations were located at one kilometre interval. A total of 127 km was covered. Both base looping and detailed stations measurements were carried out simultaneously. This was because some of the traverses were along tracks which were hardly motorable. 1:50,000 topographic maps published by the Federal Survey of Nigeria were used to locate the positions of each station. Stations were determined using the odometer of the field vehicles which had an accuracy of 0.1 km. Stations could be located on the 1:50,000 map with a precision of about ± 10 m, which causes an error of about $\pm 3 \times 10^{-5}$ g.u.

The elevations of all the stations were determined using two Wallace and Tiernam altimeters. The values were compared with contours on the topographic maps and both heights were found to be consistent to an accuracy ± 5.0 m. All the altimeter readings were tied to the only known bench mark with a height of 408.43 m, located at the Post Office in Azare.

3.2 INSTRUMENTATION:

The main instruments used for the survey were the Worden Gravity Meter and two Wallace and Tiernan Altimeters.

3.2.1 THE WORDEN GRAVITY METER:

The gravity measurements were carried out using the standard Worden gravity meter model No. 135 belonging to the Physics Department of Ahmadu Bello University. The gravimeter was transported by car or Land Rover Jeep. It was secured on a cushion seat in the vehicle. The Worden gravimeter has a fixed instrumental constant of 0.092 mgal. per division. The instrument was said to have an accuracy of about ±0.1 mgal for readings less than 2,500 mgal. Prior to the field work the instrument was placed in a room and observed for three days from 0600 - 2000 hours. This covers the period within which readings will be taken in the field, during the survey. It was observed that the drift rate of the gravimeter checked every three hours was not more than 0.10 mgal/hour (fig 4). This value is far below the manufacturers recommended maximum drift rate of 0.30 mgal/hour. The drift rate is of course an intergrated effect of the diurnal drift, temperature drift and normal drift of the gravimeter.

3.2.2 The Altimeter:

Two Wallace and Tiernan altimeters No. Fa181/mm/1911

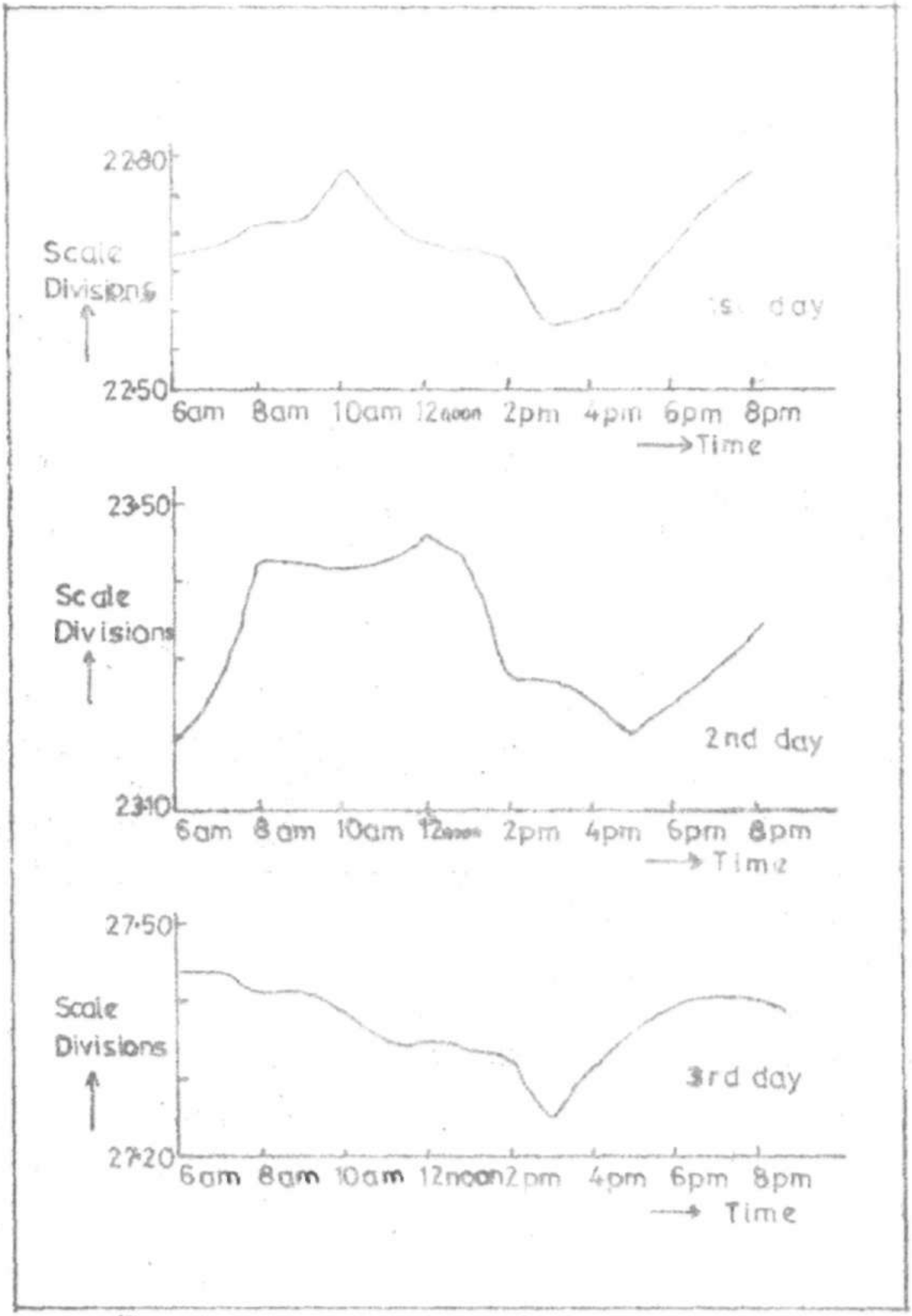

Fig. 4 GRAVIMETER DRIFT RATE CURVES.

and No. Fa181/13560 were used in the survey. These instruments are basically aneroid barometers. Each scale division on the altimeter is equivalent to ten feet (or 3.05 m). The survey altimeter readings were taken to the nearest two feet (0.61 m).

A standard pressure - altitude relationship is normally used in the calibration of an altimeter. Clendinning et. al.(1969) felt that the relationship between pressure and height was not just a simple relationship, but that it was complex. This was because pressure depended on gravity effect, air temperature and humidity.

They proposed two assumptions either of which if applied will ease the complex relationship between the pressure and altitude. The assumptions are:-

(i) that the atmosphere is isothermal, that is temperature does not vary with altitude or

(ii) that there is a constant rate of decrease of temperature with increasing altitude i.e. a constant lapse-rate.

These conditions are however very difficult to attain in the atmosphere, hence corrections are made to the observations of the altimeter for humidity, temperature, and instrumental drift, as recommended by the designers of the altimeter.

CHAPTER FOUR

FIELD MEASUREMENTS AND D.M. REDUCTIONS

4.1 Base Station Net Work:

The primary base of the survey at Azare had earlier been tied to the IGSN - 71 station at Kano, and its value was given as 9781346.5 g.u. (M.J.T. Verheijen - Personal Communication).

During the survey a total of twenty-three base stations were established, including the primary base station by the well known base looping method (Nettleton, 1971). The distance between the base stations varied from 5 km to 13 km.

The readings were corrected for drift which included the instrumental drift and tidal variations. The drift was assumed to have a linear relationship with time between two control stations. For a time interval, the drift rate between two adjacent base stations 'a' and 'b' was calculated using the relation.

$$N = \frac{(g_b - g_a) - k(R_b - R_a)}{t_b - t_a} \quad \ldots\ldots \; 4.1$$

Where N is the drift rate, g_a and g_b are the absolute values of base stations a, and b respectively, R_a and R_b are the gravity meter field readings at the times t_a and t_b respectively for the base stations a and b, and k is the instrumental constant.

The absolute value g_i of a detail station i, is given by $g_i = g_a + k(R_i - R_a) + N(t_i - t_a)$. - - - - - - 4.2. Where R_i and t_i are the gravity meter reading and time at the station i.

4.2 Elevation:

The altimeters, gravimeter and the psychrometer were read alongside one another, therefore the same base stations were used for the different measurements. The time between two base stations were kept to a maximum of three hours.

The readings of the altimeters were first corrected for air temperature and relative humidity as provided in the altimeter manual. The elevations of the base stations were determined relative to the primary base station whose height was 408.43 m. A linear drift rate of the altimeter between two base stations was assumed as was done for the gravimeter readings.

An average of the computed values of the two altimeters was found and used as the elevation of the stations. Each scale division on the altimeters is equivalent to 10 ft (3.05 m) but during the survey the scale divisions were read to the nearest 2 ft (0.61 m). The estimated error for each of the detail stations was ±1.0 m. Recent studies have indicated that in the West African Savannah area considerable reliability can be attached to the results deduced from aneroid altimeter readings due to the stability of the diurnal pressure variation. An estimated accuracy of ±1.2 m in the day during the dry season and 2.5 m in the wet season is expected (Verheijen and Ajakaiye, 1980).

4.3 Free-Air and Bouguer Anomalies:

The free - air anomaly at a station was determined using the equation

$$g_F = g_s - g_t + \frac{dg}{dR}h \qquad \text{- - - - - - - - - 4.3}$$

where g_F is the free - air anomaly, g_s is the absolute gravity at a station, g_t is the theoretical gravity value extrapolated from the reference ellipsoid and $\frac{dg}{dR}$ is the vertical gradient of gravity where R is the distance from the reference geoid to the centre of the earth and h is the height of the station above sea level.

The Bouguer anomaly at any station is determined using the equation

$$g_B = g_s - g_t + \frac{dg}{dR} h - 2\pi \rho Gh \quad - - - - - - - \quad 4.4$$

Where g_B is the Bouguer anomaly, G is the Universal gravitational constant, g_s, g_t are as in equation 4.3, and ρ is the mean crustal density. ρ is the assumed crustal density of the earth.

g_s, g_t, $\frac{dg}{dR}$ and h are same as in equation 4.3.

The vertical gradient of gravity

$$\frac{dg}{dR} = - (3.096 + 0.002297 \cos\phi) \text{ g.u/m.} \quad - - - - \quad 4.5$$

(Grant and West, 1965).

The latitude effect can be corrected for by using the theoretical value g_t which is given by

$$g_t = g_o \,(1 + A\sin^2\phi) + B\sin^2 2\phi) \quad - - - - - - \quad 4.6$$

(Telford et. al 1979).

where g_o is the equatorial gravity given as 9780318 g.u. and ϕ, A, B are the latitude, 0.0053024, and - 0.0000058 respectively.

The Bouguer correction is applied to remove the effect of an assumed infinite slab (the material between the horizontal plane of each station and the sea level) which is $2\pi\rho$ Gh, where ρ and h are as in equation 4.4.

This value is 1.118997 h, where h is the height of the station above sea level in metres.

Possible sources of error in the elevation, Bouguer anomaly or free-air anomaly include the non linearity of the drift rates and gravimeter, the precision of the instruments and accurate location of field positions on the topographic maps which affect the value of the latitude corrections. The non linearity of the drift rates contributed an error of about ±1.5 g.u., the precision of the instrument contributed an error of about ±0.9 g.u. while contribution by locating of field position with difference of ±0.5° has an error of less than ±2 g.u. The elevation has an error of +1.5 m. This error in the elevation will cause errors of ±2.5 g.u. and ±1.9 g.u. in the free air and Bouguer anomalies respectively.

The total errors in each determination of the Bouguer anomaly at any given station is about ±5.4 g.u.

CHAPTER FIVE

DENSITY MEASUREMENTS

5.1 Introduction:

The gravity exploration method primarily detects horizontal variations in the densities of rocks buried beneath the ground surface. Therefore to attempt any meaningful quantitative interpretation of gravity data, the densities of the dominant rock types in the area must be determined. Besides, geophysical data interpretations very much depend on the physical properties of rocks.

Samples from various parts of the complex were collected and carefully labelled in order to obtain as much factual information as possible on the densities of the rocks in the area.

5.2 Sample and Identification:

A total of forty nine samples were collected at different gravity stations within the complex. These samples were knocked off from outcrops and as much as possible only fresh samples were collected.

Dr. E.C. Ike of the Geology Department of Ahmadu Bello University Zaria helped to identify and to classify the rocks.

They include:-

12 samples of aegirine arfvedsonite alkali feldspar granite, 13 samples of annitic biotite alkalifeldspar granite, 10 samples of ferrorichterite - arfvedsonite alkali-feldspar granite, and 14 samples ferrorichterite arfvedsonite aenigmatite alkali feldspar syenite.

5.3 Density Measurements:

It is often not easy to obtain accurate bulk density value from rock samples because of the difficulty of finding fresh unweathered samples as fragmentation and or dehydration, invariably have acted on the surface outcrops. Also in situ density measurement was not possible because of lack of bore hole in the complex area. However a fair approximation to the in situ density is usually obtained by averaging the dry and saturated laboratory density measurements (Parasnis, 1976).

All weight measurements in the density determination were done with the Electronic balance No. 15. In both the dry and saturated density determinations the

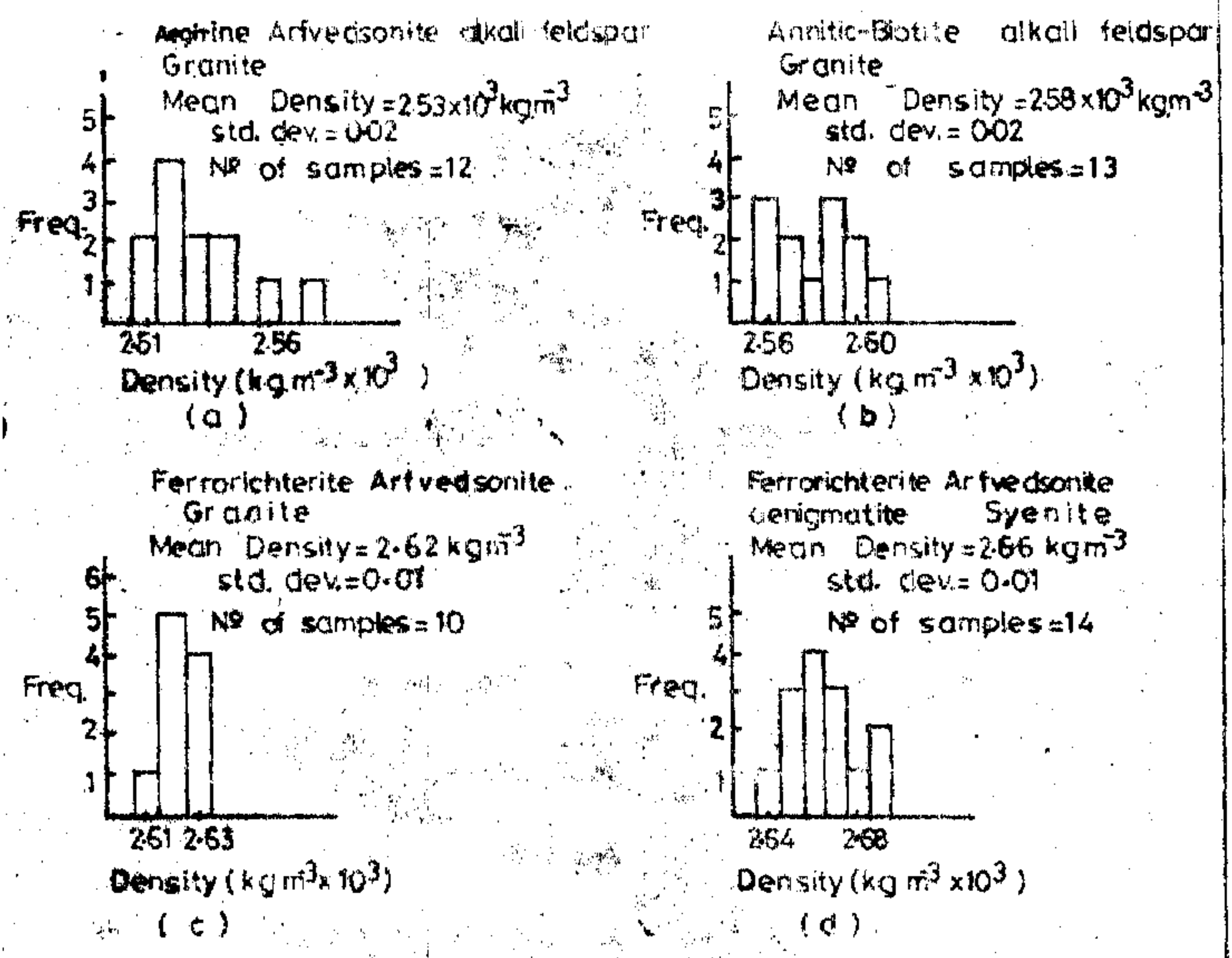

Fig 5 DENSITY HISTOGRAMS OF ROCK TYPES.

rook samples were weighed in air and when completely immersed in water. To achieve saturation of the rock samples they were immersed in water for 48 hours.

The density of any material is given by

$$P = \frac{Wa}{W_a - W_w} \quad - \quad - \quad - \quad - \quad - \quad 5.1$$

Where W_a is the weight of the material in air and W_w is the weight of the material when completely immersed in water whose density is 1×10^3 kg m^{-3}.

5.4 Error in the Density values:

The "electronic" metter balance is accurate to about 1×10^{-3} kg. The rock samples oollected range in mass from about 0.3 kg to about 6 kg. The error in the density determination of each sample would be about 2×10^{-4} kg m^{-3}.

Table I summarizes the results for the densities of the rock types encountered in the area. The difference between the wet and dry densities was less than 0.8 per cent.

Table 1 DENSITY OF ROCK TYPES

ROCK TYPES	No of Samples	Range of Densities $x10^3 kg\ m^{-3}$	Average Density $x10^3 kg\ m^{-3}$	Standard Deviation $x10^3 kg\ m^{-3}$
Aegirine-Arfvedsonite Alkali Feldspar Granite	12	2.51-2.58	2.53	0.02
Annitic-Biotite alkalifeldspar Granite	13	2.56-2.61	2.58	0.02
Ferrorichterite Arfvedsonite Alkalifeldspar Granite	10	2.61-2.63	2.62	0.01
Ferrorichterite Arfvedsonite aenigmatite alkali feldspar Syenite	14	2.64-2.69	2.66	0.01

The value of the densities of the different rock types agree with the results of earlier researchers (Ajakaiye, 1975; Amosu, 1980). Histogram was plotted for each rock type (fig. 5). The density values of 2.53, 2.58, 2.62, 2.66 x 10^3 kg m^{-3} obtained for aegirine-arfvedsonite granite, annitic - biotite granite, ferrorichterite arfvedsonite granite, and ferrorichterite arfvedsonite syenite may not truely represent the actual density of the rocks, in situ, due to differences in compactness, and liquid content at various depths. Hence the mean of the dry and wet densities was considered as an approximation of the "true" density of the rock.

CHAPTER SIX

INTERPRETATION OF GRAVITY DATA

6.1 The Description of the Bouguer Anomaly Map:

The Bouguer anomaly shown in fig. 6 was produced by contouring the Bouguer anomalies calculated for each station occupied during the survey. The contour values range from - 100 g.u. to - 330 g.u. and the contour interval is 10 g.u.

An inspection of this map will reveal that there are three major anomalous centres, two of which are positive and one negative, labelled A, B and C respectively. The positive anomalies have a NE - SW trend with the negative anomaly located to the SE end.

The positive anomaly A occupies an area of about 370 km^2 at the northern section of the area under investigation. The contour values range from - 110 g.u. to - 230 g.u. The pattern of the contours is pear-shaped striking SW with its centre located off Shira along its strike.

The positive anomaly B has a circular shape occupying an area of about 177 km^2 at the south-western corner of the area. The contours range from -100 g.u. to -240 g.u.

The pattern of the negative anomaly C is more complicated compared with the rather simple anomalies A and B. It has an E - W trend with contours ranging from - 330 g.u. to - 260 g.u. This anomaly occupies an area of about 260 km^2.

The locations of the outcropped ring complex coincide with the locations of the positive anomaly A at the northern part and a negative anomaly C at the southern part.

6.2 The Regional and Residual Anomaly separation:

6.2.1. The Regional Anomaly Map:

Anomalies of interest in gravity interpretations of most cases are masked by deep seated structures such as the basement complex. The separation of residual anomaly by fitting the regional anomaly on the Bouguer anomaly continues to constitute a major problem in the interpretation of gravity data.

There are two main ways by which a regional map can be arrived at. These are through graphical and analytical methods. Unfortunately none of the known methods can produce a unique solution. Nettleton (1954); Dean, (1958) and Roy. (1966) have pointed out that different formulae for the analytical method give quite different numerical results and different grid spacings give different results with the same formula. The degree of reliability of the graphical method depends on three main factors; personal judgement of the interpreter, geological background and all the geological theories and assumptions he accepts or develops (Vajk, 1954).

Where the survey is of local nature requiring few data set, graphical method have been found to give good results (Telford et al., 1979). This is the case in the present survey. Consequently graphical methods have been used and found successful.

The geology of this area has been mapped in detail (Bennett, 1981). Some gravity work had also been done around this area (Ajakaiye and Burke, 1972); these indicate values of about - 300 g.u. in the northern and eastern parts.

An initial regional map was generated using the regional trend of the Bouguer anomaly map of Nigeria by Ajakaiye and Burke (1972). Six profiles were taken at

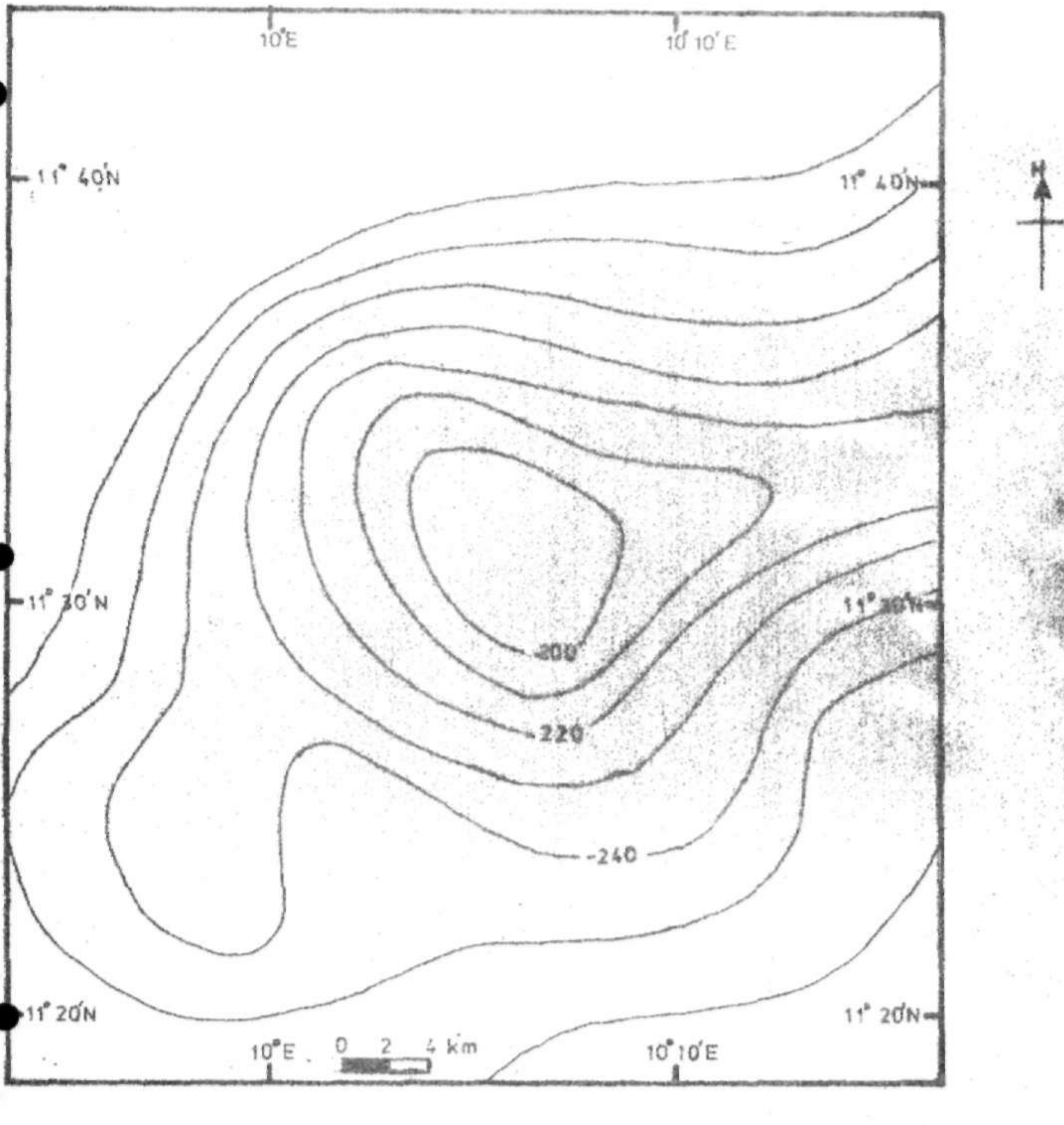

Fig. 7 Map of the Regional Gravity Anomaly.
(Contour interval 10 g.u)

random over this map. The anomalies were smoothen and the resulting curve were plotted and contoured to give the regional anomaly map of the area (fig 7). Theoretically, the regional anomaly (map) is what one removes from the observed anomaly in order to make what is left look like the structure (Nettleton, 1971). Even though this is often or probably the case, there is always a check on what can be considered as an acceptable regional anomaly map of an area. For example, a regional anomaly should have least correlation with the elevation map (Grant and Elsaharty, 1962). A correlation test along the profiles gave an average correlation coefficient of - 0.06. This result implies very low correlation between the regional map obtained and the elevation. Hence the regional gravity map (fig 7) produced through this visual smoothening was assumed to be representative of the regional anomalous features of the area, and was therefore used to produce the residual map shown in fig. 8.

6.2.2 <u>The Residual Anomaly Map</u>:

The contour values on the residual map range from - 70 g.u. to 140 g.u. (fig 8). There are two distinct positive anomalies on this map, which have a NE - SW trend

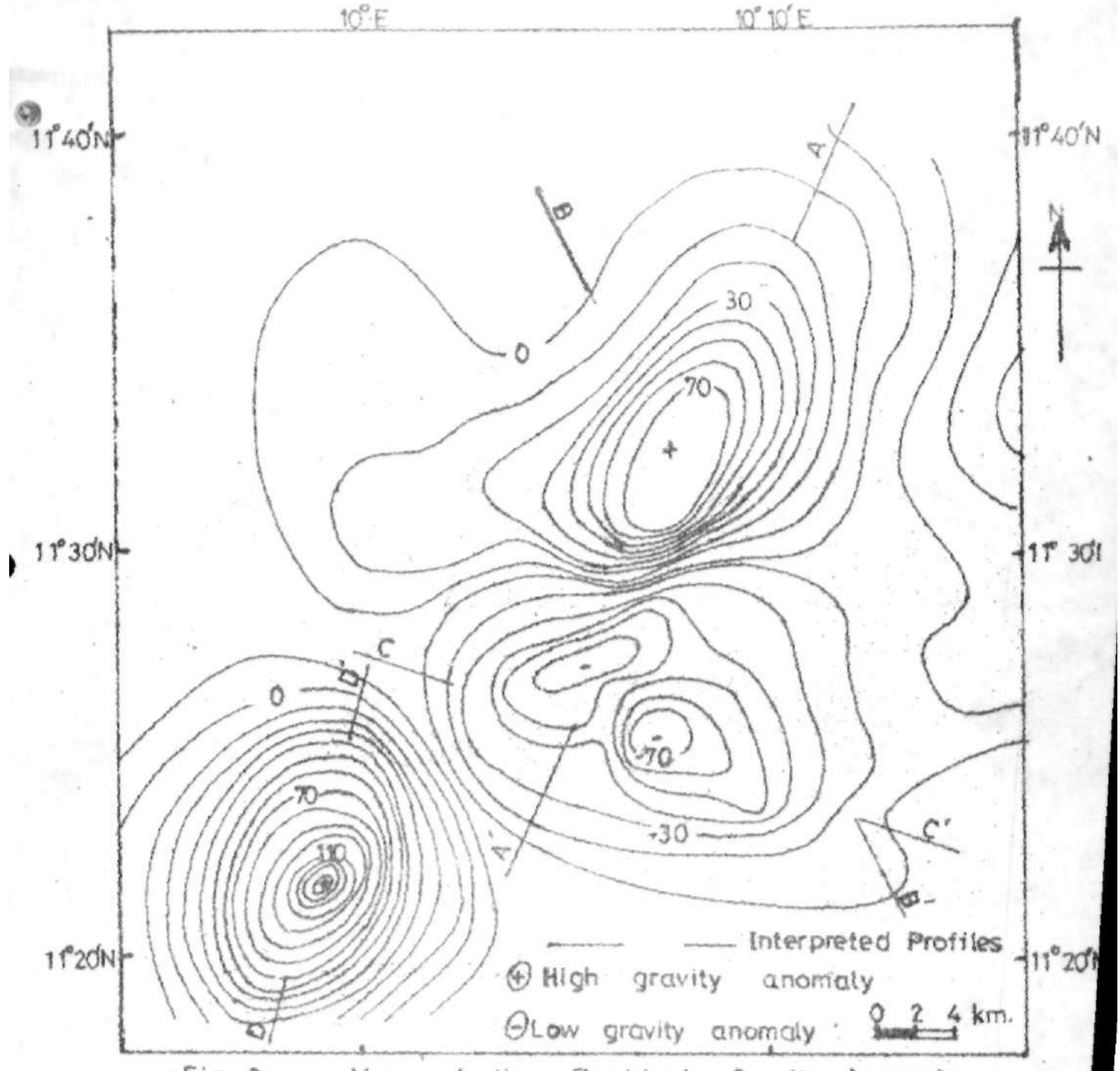

Fig. 8 Map of the Residual Gravity Anomaly
(Contour interval 10 g.u.)

with contour values ranging from - 10 g.u. to 70 g.u., and -10 g.u. to 140 g.u. respectively.

A major negative anomaly is located in the central part of the map with contour values ranging from - 70 g.u. to - 10 g.u.

6.3 The Qualitative Interpretation:

6.3.1 The Profile AA' (NE - SW):

The profile AA' extends from Azare (NE end) through Shira to Yana and beyond in the SW direction and covers a distance of 46 km (fig. 9). The negative residual values at the NE end of the profile correlate with the geological observation that Azare is located in the Chad Basin (fig 1). The residual gravity anomaly values gradually become more positive as the profile approaches the Younger Granite ring complex, and attain a maximum value of + 70 g.u. over the northern part of the ring complex.

Negative gravity anomalies have been associated with Younger Granites instrusions within the basement complex (Ajakaiye, 1968, 1970, 1974, 1975; and Amosu, 1980), and acid plutons over the country rock in general (Bott, 1953, Bott and Smithson, 1967). The most probably cause of the

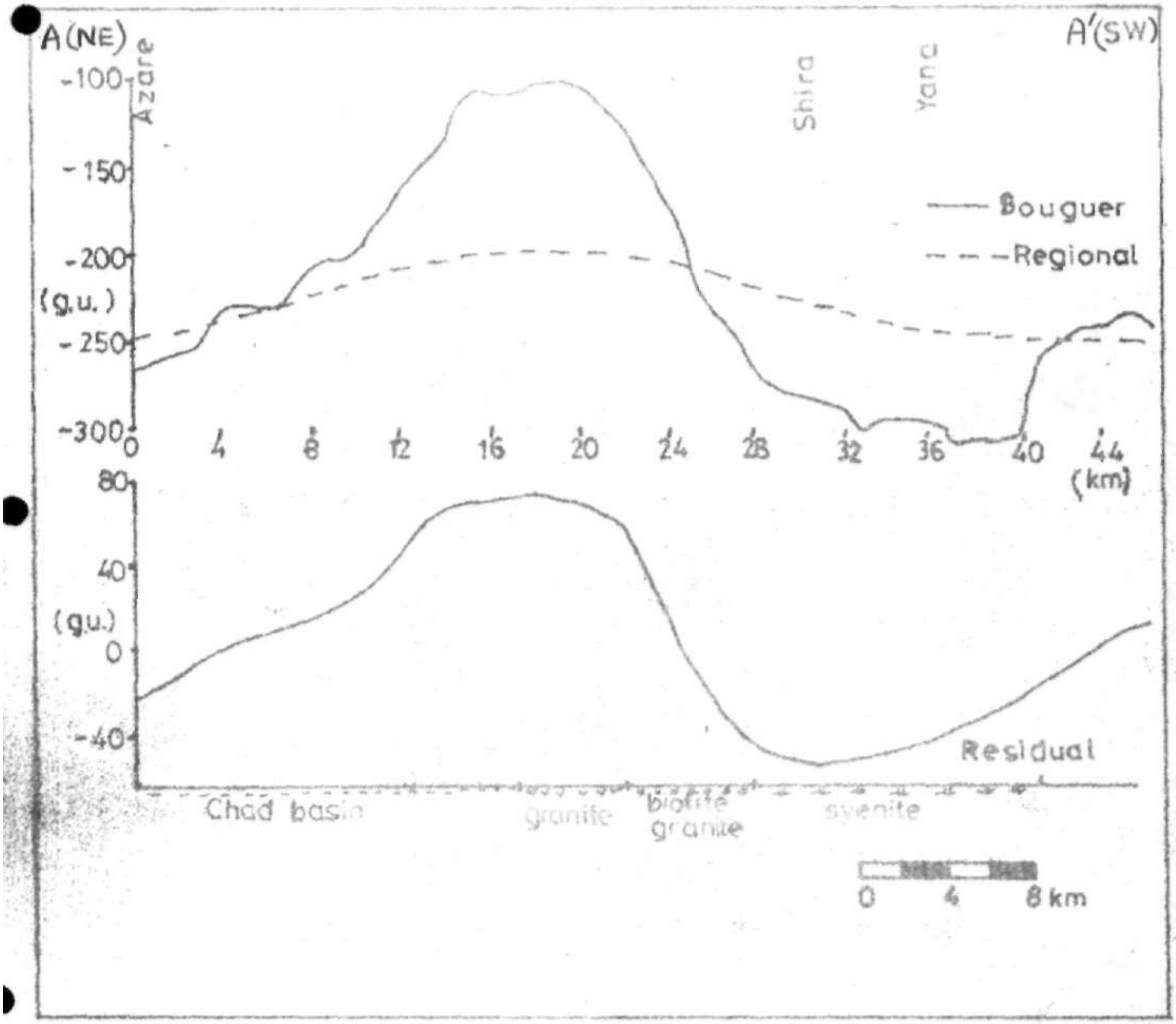

Fig.9 THE GRAVITY ANOMALIES OF PROFILE A A′.

observed positive gravity anomaly at the NE end of the profile AA' is an unexposed intrusion of a high density material within the Younger granite complex, while the observed negative gravity anomaly along the profile is probably the intrusion of the Younger granite ring complex (Syenitic rock type exposed) within the basement complex at the SW end.

6.3.2 The Profile BB' (NW - SE):

This 40 km profile runs along a NW - SE direction across the complex passing through Shira (fig. 10). The observed residual gravity anomaly along this pfofile BB' is similar to that observed on profile AA' (fig. 9). The positive anomaly of amplitude + 70 g.u. is also observed over an exposed arfvedsonite granite and biotite granite of the Shira younger granite complex. The pattern of the observed residual anomaly does not obviously correlate with the local geology which is similar to profile AA'. It is obvious therefore that this positive anomaly is possibly due to a high density intrusive buried at shallow depths within the Younger granite at the NW end, as in profile AA'. The negative residual gravity anomaly observed at the SE end of this profile BB' across the

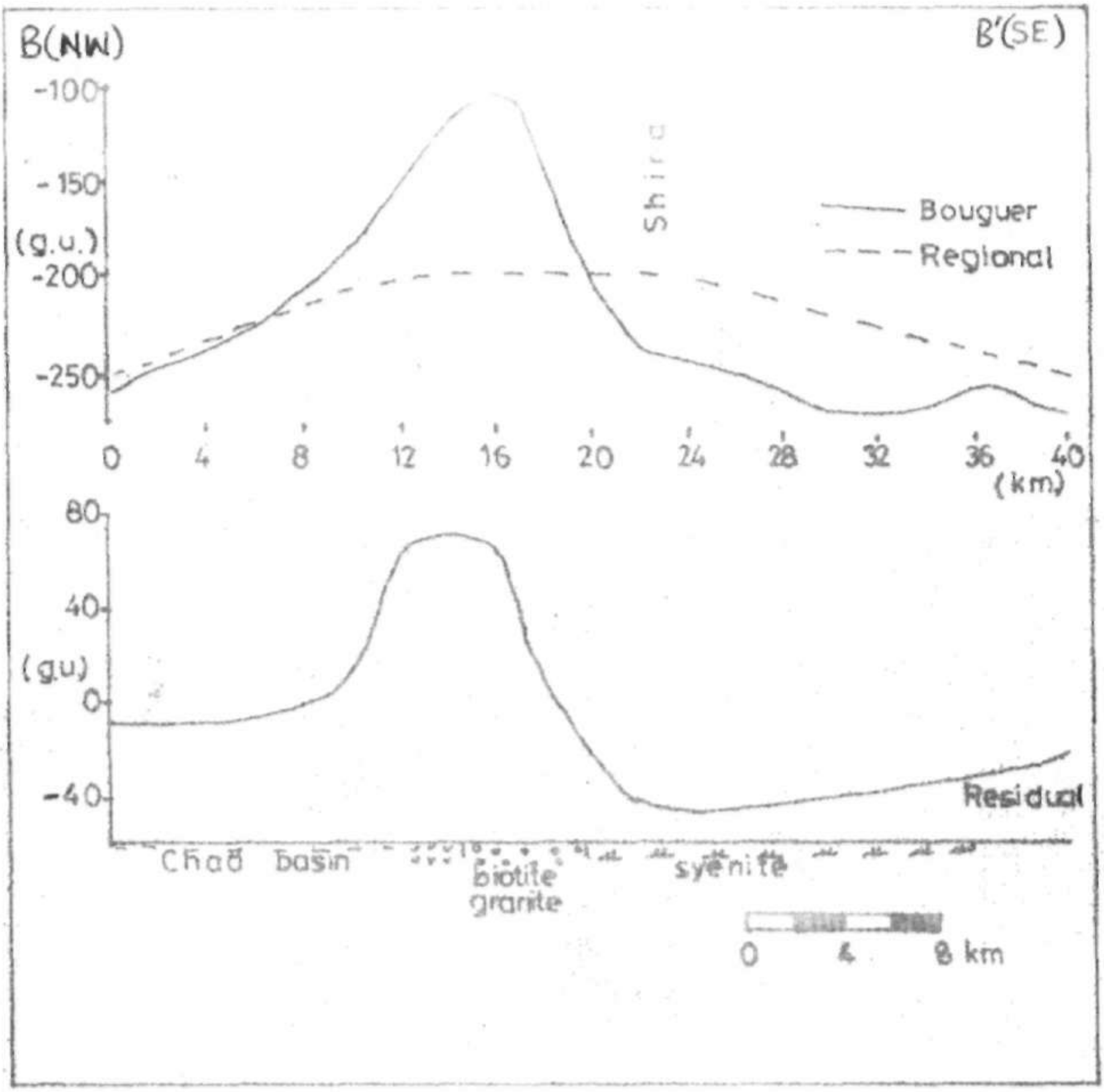

Fig.10 THE GRAVITY ANOMALIES OF PROFILE B B'

aenigmatite alkali-feldspar syenite is expected since the density of the syenitic body is lower than that of the basement rocks.

6.3.3 The Profile CC' (WNW - ESE):

This 43 km profile runs across Yana in a WNW - ESE direction (fig. 11). The residual anomaly shows a central minimum of amplitude - 85 g.u. This negative residual gravity anomaly correlates with the exposed ferroriwinchterite/ferrorichterite arfvedsonite aenigmatite alkali - feldspar Syenite which intruded the basement complex rocks in this area.

6.3.4. The Profile DD' at the SW corner (N-S):

This N-S profile (fig. 11) is located at the SW corner of the area under investigation (fig. 8). It is 18 km long and was isolated for interpretation because of its large positive anomaly observed.

Since no outcrop is observed along the profile which is located on the apparently homogeneous basement complex (Bennett, 1981) the causative body is proposed to be an intrusion of a high density body buried at shallow depths within the basement complex (Bott, 1953). The density of this buried high density body is assumed to be the same as

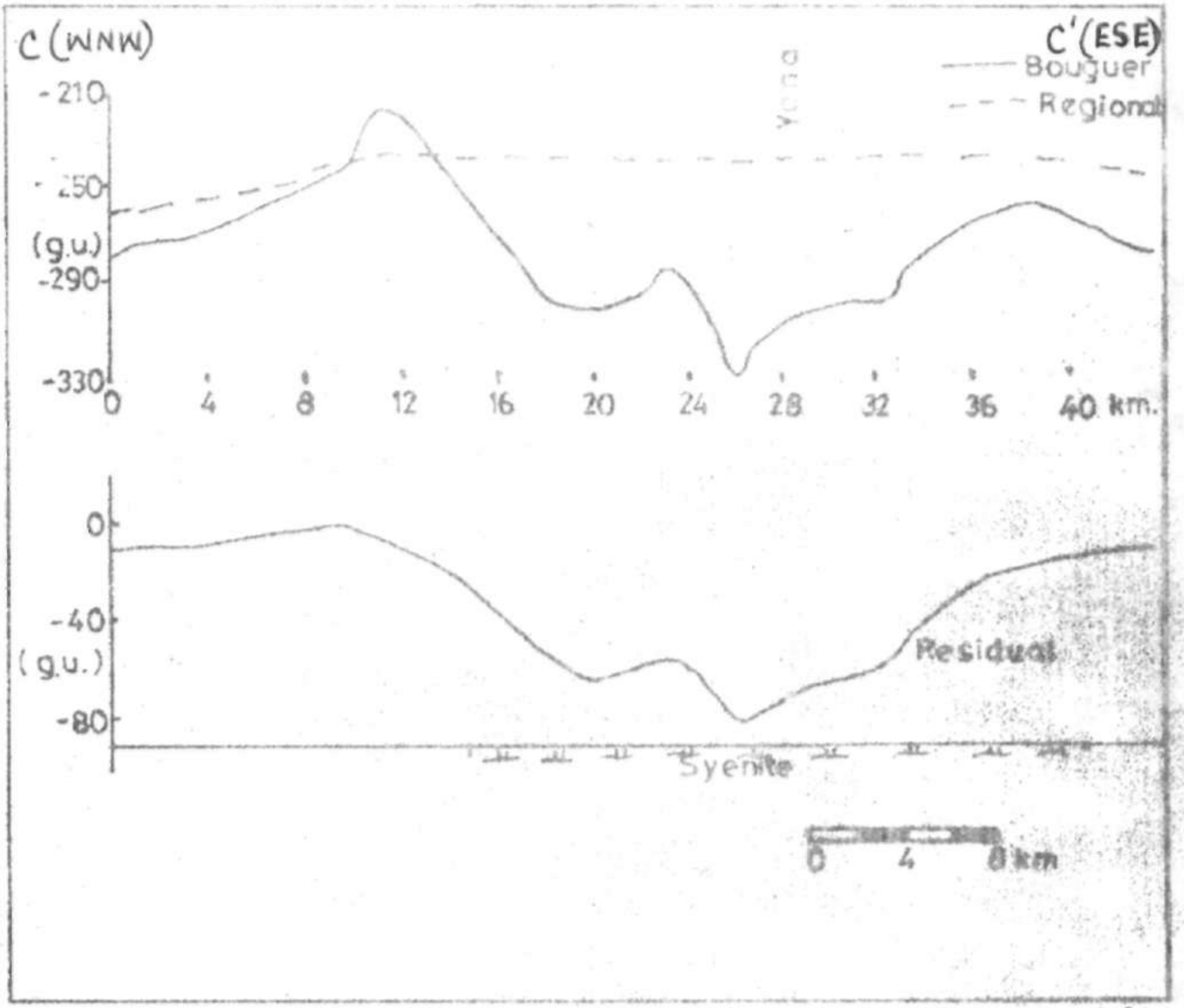

Fig. 11 THE GRAVITY ANOMALIES OF PROFILE CC'.

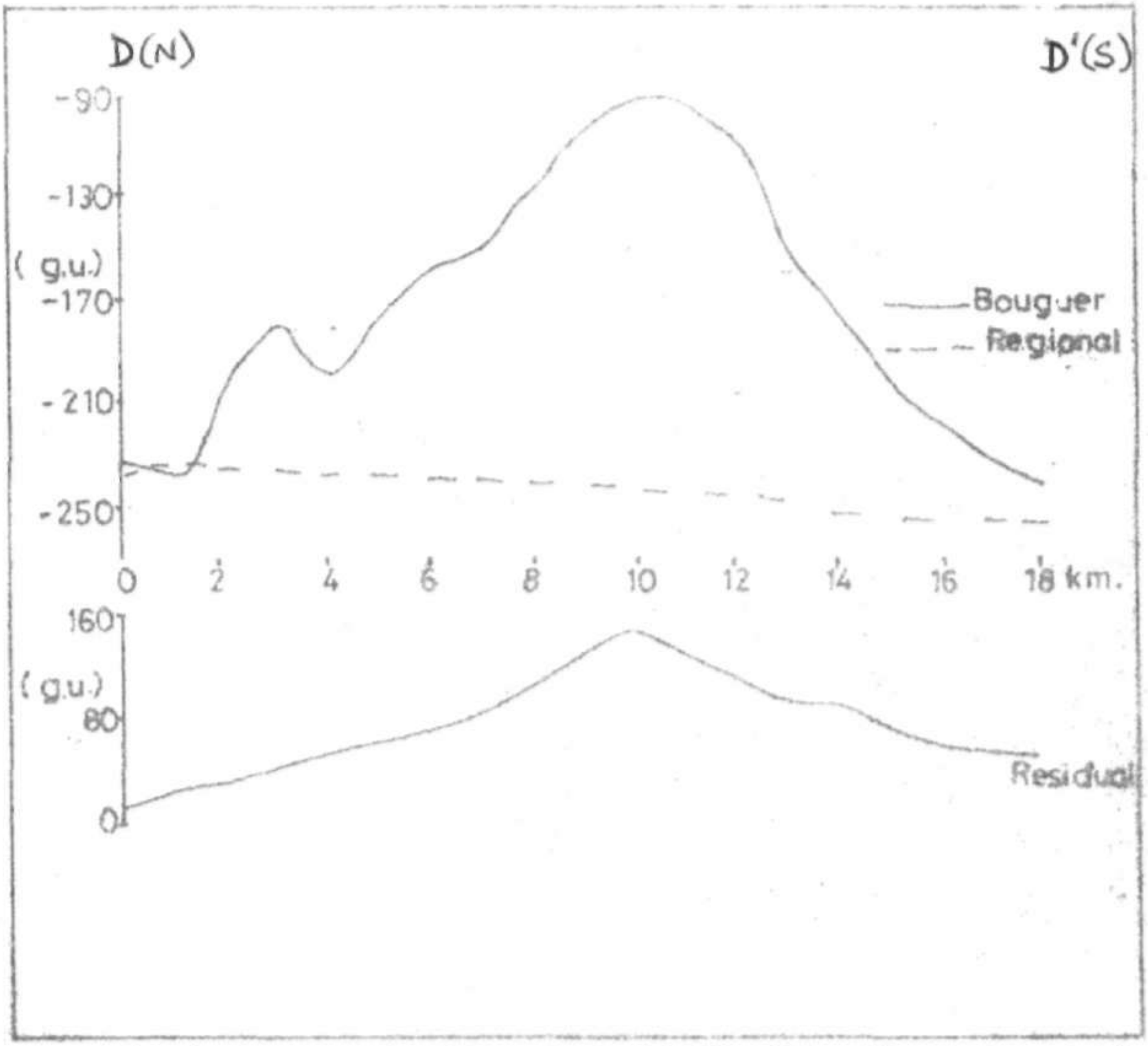

Fig.12 THE GRAVITY ANOMALIES OF PROFILE D D'.

that proposed in the pfofiles AA' and BB'.

6.4 Quantitative Interpretation:

6.4.1 Introduction:

The usual objective of quantitative interpretation is to calculate the depth, size and shape of the body causing the gravity anamaly (Grant and West, 1965). Often there is an erroneous assumption that the calculated body is a unique solution to the cause of the observed gravity anomaly. Whereas a buried mass with a specified position, shape and density will give rise to a predictable gravity field on the surface, any observed gravity field could be produced by an infinite number of possible mass distributions (Dobrin, 1976). This non-uniqueness in the interpretation of potential field data not withstanding, indirect method of modelling is used in interpretation of gravity data. This involves postulating several models of bodies based on density and geological considerations, and calculating their gravity effects. The calculated fields of each model is compared with the observed anomalies and the model that gives the best fit is assumed to represent the causative body.

6.4.2 Modelling:

A two-dimensional interpretation was attempted along four profiles (AA', BB', CC' and DD'), two of which were almost at right angle to each other. These profiles run across prominent anomalies on the Bouguer anomaly map (fig. 6) and the Residual anomaly map (fig. 8), and in most cases these profiles coincide with the field traverses.

In modelling the causative bodies beneath the profiles, available geologic informations such as the geologic boundaries, the average dips of the beds were used in constraining the models. The intrusive body and other rock formations were assumed to be homogeneous, and therefore has a constant density.

The density values determined in chapter five were employed in the modelling. The syenite, arfvedsonite alkali feldspar granite and the aluminous biotite granite have densities of 2.66, 2.62 and 2.58 x 10^3 kg m^{-3} respectively, and these values are comparable with the density values got by Ajakaiye (1968, 1974, 1975). The density of the Chad Basin formation was taken as 2.4 x 10^3 kg m^{-3} (Myada, 1978). Due to lack of outcrops of the basement complex no samples were collected, however, the usually acceptable density 2.67×10^3 kg m^{-3} of the basement rock was taken, and this is the value used by earlier researchers (Bott and Smithson, 1962; Ajakaiye, 1968).

Bott and Smith (1958) proposed formula for calculating the maximum depth of the basement structure was used as a guide in the initial model.

In the modelling, the anomalous body was assumed to be irregularly shaped and its cross-section is represented by a polygon with finite number of sides. The density contrasts of the different geologic rock types with respect to the surrounding bed rock (basement complex) was fixed and the coordinates of their corner points were adjusted until the calculated anomaly fit approximately the observed anomaly.

The modelling was facilitated by using a computer programme developed by Nagy (1964) and adapted by Ojo (1974) to suit the computer of the Ahmadu Bello University.

6.4.3 The Interpretation of the Profiles:

(a) The Profile AA' (NE - SW):

Two distinct residual anomalies, one positive and the other negative (fig. 13) are no doubt

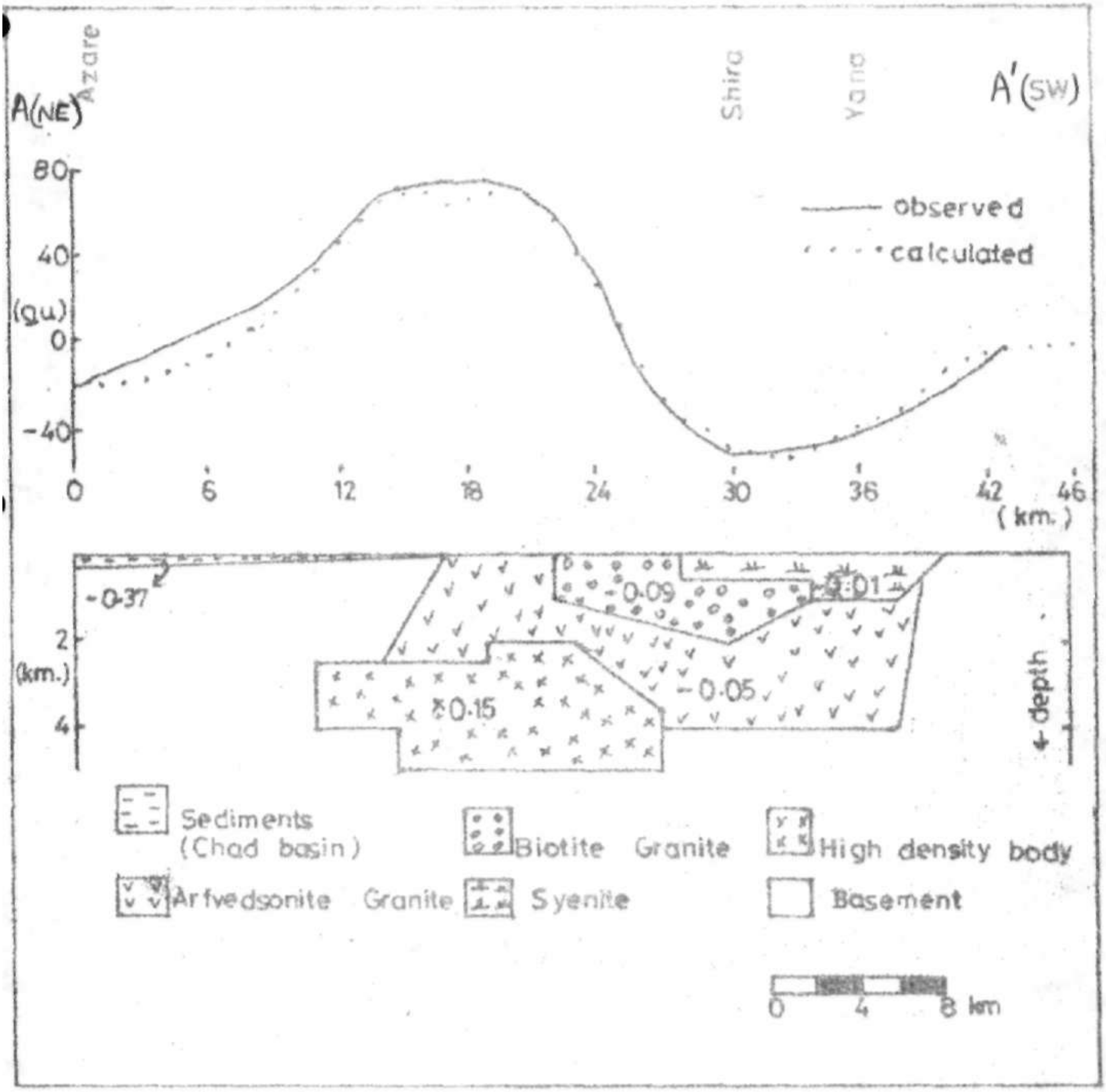

Fig 13 TWO DIMENSIONAL STRUCTURAL MODEL OF PROFILE AA'.

of interest. The positive anomaly has already been suggested to be due to an unexposed intrusion of a high density material within the Younger granite. The negative anomaly at the NE end of the profile has also been attributed to the sediments of the Chad Basin, while the minimum at the SW end is possibly due to the effect of the exposed Younger granite intruding the basement complex.

Several models were proposed and the model that gave the best fit is drawn in fig. 13. The sediments dip gently at an angle of 2^{o} to the horizontal away from the basement. The contact between the sediments and the basement along this profile is located at 17 km NE of Azare.

The observed positive anomaly across the arfvedsonite granite and part of the biotite granite (fig. 13) is interpreted as being due to these two bodies, whose density contrasts are observed from the surface, to depths of between 2.5 to 4 km and 1.0 to 2.0 km. respectively. The arfvedsonite granite is exposed between 17 and 22 km from the NE end of the profile while the biotite granite is exposed between 22 and 28 km. A high density body, possibly a basaltic plug is buried at depth between 2.0 km and 5 km and is 17 km wide. The aenigmatite syenite overlies the biotite and the arfvedsonite granite layers and it extends to depths between 0.5 km to 1.0 km and is exposed between 28 km and 40 km from the NE end of the profile.

(b) The Profile BB' (NW - SE):

Similar to profile AA', profile BB' has two distinct residual anomalies of interest. In the model (fig. 14) for the observed anomalies along this profile the Chad Basin is at the NW end and has sediments dipping gently at an angle of 3^{o} to the horizontal away from the basement, and is underlain by the basement complex. The contact between the sediments and the basement along this profile is located at 12 km from the NW end. The positive anomaly observed across the arfvedsonite and the biotite granite is interpreted to be due to a high density body possibly basaltic plug buried at depth 1.5 km within the arfvedsonite granite, and has a lateral extent of 9 km. The arfvedsonite granite

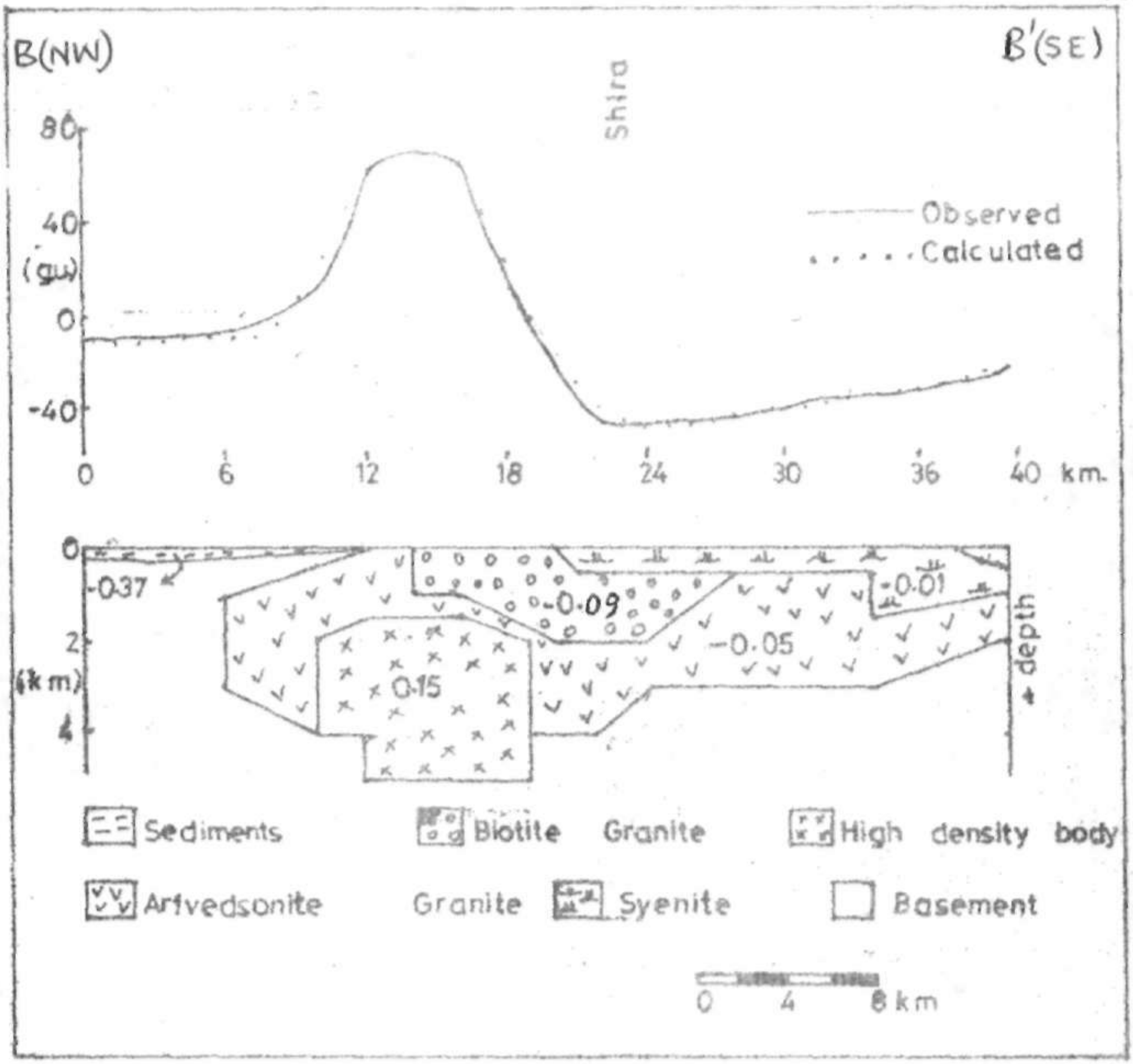

Fig.14 TWO DIMENSIONAL STRUCTURAL MODEL OF PROFILE B B'.

density contrast is observed from the surface to a depth of 4 km and has a lateral extent of over 34 km. Overlying the arfvedsonite granite is the biotite granite, and is exposed from 14 km to 20 km from the NW end (fig. 14) The syenitic. layer overlies the biotite granite and is exposed from 20 km to the SE end of the profile.

(c) The Profile CC' (WNW - ESE):

The main rock type exposed along this profile is syenitic, which belongs to the younger granite group of rocks. An initial interpretation assuming the profile is underlain solely by syenite and basement rocks can be calculated to approximate the observed gravity anomaly. A body of thickness much greater than 8 km is required if the surface density contrast between the syenite and the basement (0.01 g/cm^3, Table 1) is used in the calculation. This thickness far exceeds the calculated models for other ring complexes within the younger granite province (Ajakaiye 1973, 1974; Amosu 1980). Since this profile CC' cuts across the same younger granite complex, the interpretation of the other profiles

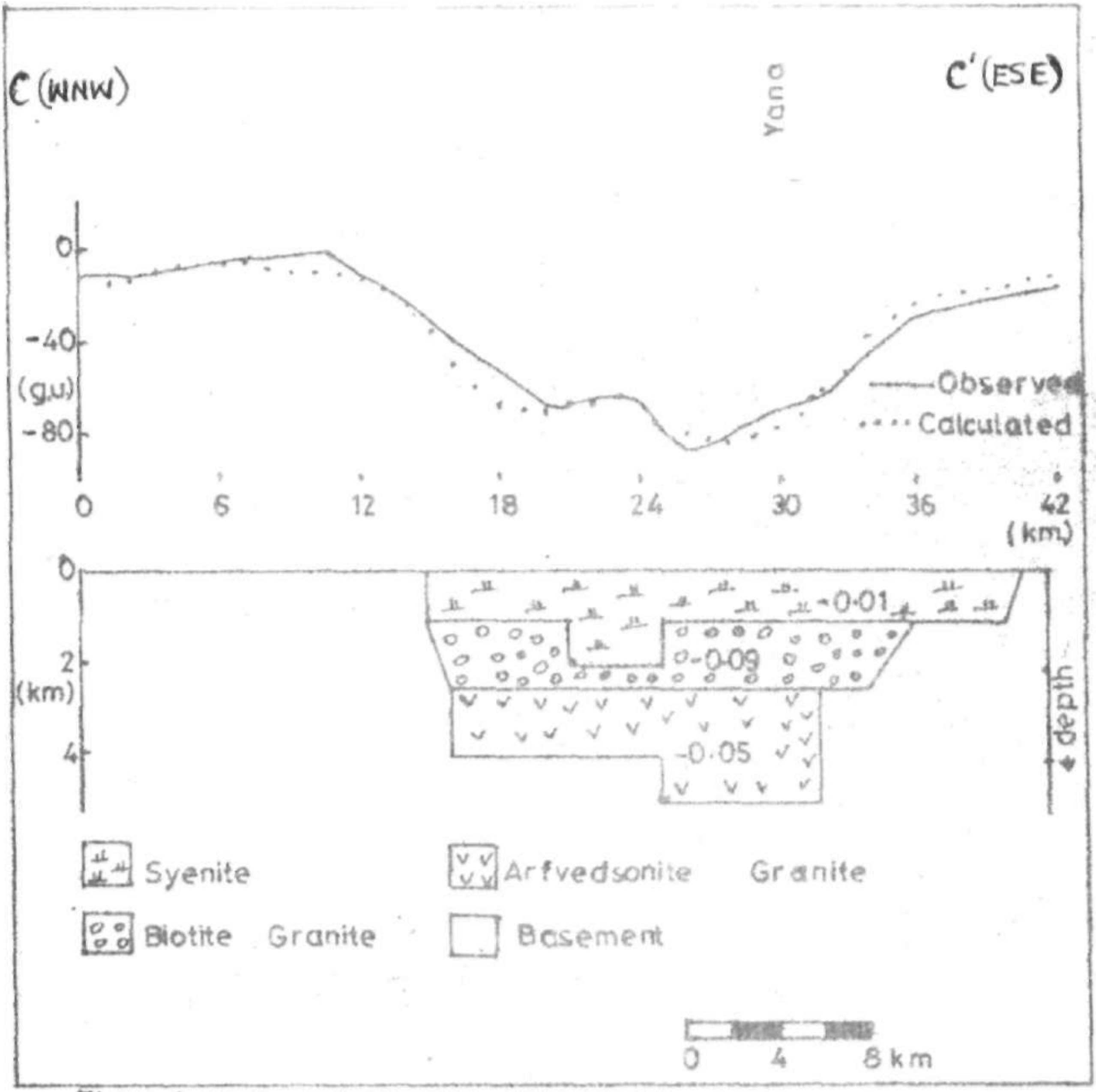

Fig 15 TWO DIMENSIONAL STRUCTURAL MODEL OF PROFILE CC'

along which the other rock types of the complex are exposed will influence the choice of a suitable model. Hence the layering exhibited in the models of profiles AA', BB' is considered to be likely in this profile CC' (fig. 15).

In the model with the best fit, the syenite has a maximum depth of 2 km with a lateral extent of 30 km and overlies the biotite granite. The biotite granite is at depth between 1.5 km and 2.5 km with a lateral extent of 22 km and is underlain by the arfvedsonite granite. This arfvedsonite granite is buried at depth between 2.5 km and 5 km with a lateral extent of 16 km.

(d) The Profile DD', (SW corner, N - S):

The profile DD' located at the SW corner is the only profile which does not cut across any outcrop.

A proposed model which fits the observed gravity anomaly shown in fig 16 is a body which intruded the basement. The depth to the surface of this intrusion varies from 0.5 km to 2 km. At a depth of about 2 km and 3 km there is a lateral spread extending to 15 km. This body is suspected to be basaltic.

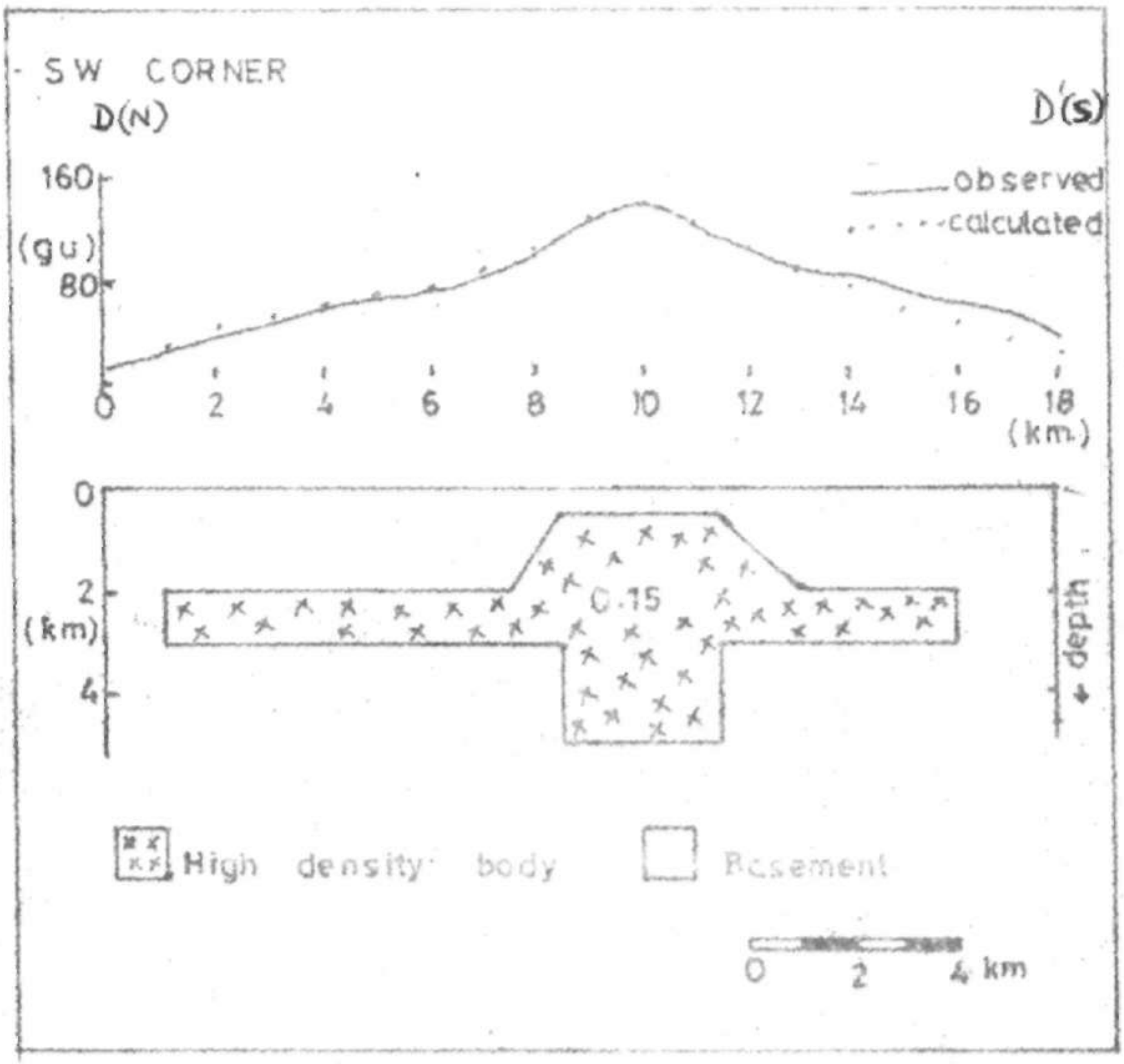

Fig.16 TWO DIMENSIONAL STRUCTURAL MODEL OF PROFILE DD'.

CHAPTER SEVEN

DISCUSSION AND CONCLUSION

7.1 Discussion:

An accurate estimation of the regional gravity anomaly trend is significant in the interpretation of observed Bouguer gravity anomalies in a given area. In this survey area the regional trend could not be easily deduced from the observed Bouguer gravity anomalies because the area is underlain by three distinct groups of rocks, the Chad formation, at the north, the younger granite (complex of interest) and the basement complex at the south (Bennett, 1981). Both the Chad formation (sediments) and the younger granite exhibit negative gravity anomalies because of their negative density contrast with respect to the basement complex. The regional trend was therefore deduced from earlier work in the area (Cratchley and Jones, 1965; Ajakaiye and Burke, 1972; Ajakaiye and Verheijen, 1977.

Gravity anomalies are greatly influenced by densities of the rock types in situ, hence emphasis is placed on the density values used in interpretation. An attempt was therefore made to collect a truly representative sample of the rock types in the area for density determinations. The density values obtained for each rock type, used for interpretation compare favourably with values obtained by earlier workers (Ajakaiye, 1970, 1974, 1975; Amosu, 1980).

The observed residual anomalies along the profiles generally correlate with the surface geology. For example at the NE and NW ends the negative anomalies are observed across the Chad Basin. While the southern ends of the profiles correlate with the basement complex.

The intense positive anomalies observed along the profiles AA', BB' and DD' which show no correlation with the surface geology have been attributed to high density bodies intruding at relatively shallow depth of more than 0.5 km.

Although the arfvedsonite granite, the biotite granite and the Syenite are exposed at various locations (e.g. profiles AA', BB') of the younger granite ring complex it would appear that at certain locations at depth the syenitic rocks are underlain by the biotite granite and this biotite granite is underlain by the arfvedsonite (fig. 13, 14 and 15). The arfvedsonite granite though sparse in exposure, extends to greater depths (4 km) than any of the other rock types in the younger granite complex and the lateral extent is over 30 km. Some outcrops located about

10 km west of the main complex is identified as arfvedsonite granite. The biotite granite is also sparse in exposure but extends to depth of about 2 km with a lateral extent of about 12 km along the profiles (fig. 13, 14 and 15). The syenitic rocks are massive in exposure but shallowest as suggested by the models (fig. 13, 14 and 15), and the lateral extent is of average 15 km.

The usual 'knife edge' sharp contacts between various rock types of the younger granite province that were emplaced after considerable time interval (Turner, 1963) exists between the biotite granite and syenite. Besides, there is a marked density contrast between the two rock types (biotite granite and syenite) and the syenite overlies the biotite granite. These facts suggest that the syenitic rock were emplaced before the biotite granite. But there is no sharp contact between the arfvedsonite granite and the biotite granite and the density of the arfvedsonite granite is greater than that of biotite granite. Above reasons suggest that the arfvedsonite granite was emplaced soon after the emplacement of the biotite granite. This proposed order of emplacement agrees with those observed in other ring complexes in the younger granite province (Turner 1963, 1972, 1973).

A high density material, possibly basaltic in nature is postulated to intrude the arfvedsonite granite (fig 13, 14) and the basement complex (fig 16) at depth. This intrusive appears to be confined within the arfvedsonite granite, and possibly does not extend to the other rock types of the ring complex. The proposal that the high density material is basaltic appears reasonable since basalt outcrops at some 5 km beyond the Shira Younger granite ring complex at the western section of the area under investigation (Bennett, 1981).

7.2 Recommendations:

It is recommended that:

(a) Seismic method be employed to confirm the depth extent of the three main rock types in the Shira young granite ring complex.

(b) In situ density determination be carried out to give a more representative density values of the various rock types when boreholes are available.

(c) A geochronological study be carried out to test the layering hypothesis postulated in the models.

7.3 Conclusion:

1. The mean densities of the various rock types in the Shira Younger granite ring complex are: arfvedsonite granite, 2.62×10^3 kg m^{-3}, biotite granite, 2.58×10^3 kg m^{-3}, and syenite, 2.66×10^3 kg m^{-3}.

2. A high gravity anomaly is observed over the northern part of the Shira younger granite ring complex, which is caused by a basaltic intrusion within the younger granite. At the southern part of the younger granite complex a low gravity anomaly is observed which is typical of the younger granite province.

3. The gravity interpretation suggests that the different younger granite rock types that form the plutonic intrusion of the Shira complex form a layering at depth with least exposed, arfvedsonite granite being the most deeply seated while the highly exposed, syenite is the shallowest.

APPENDIX I

PRINCIPAL GRAVITY PARAMETERS OF STATIONS

1	2	3	4	5	6
Station Number	Latitude	Height (m)	Absolute Gravity (g.u)	Free Air Anomaly (g.u.)	Bouguer Anomaly (g.u.)
P.O.Azare	11° 40.45'N	408.43	9781346.5	179.5	-277.5
Km 1	11° 40.60'N	405.18	9781364.4	186.4	-267.0
Km 2	11° 40.11'N	401.88	9781374.5	189.2	-260.5
Km 3	11° 39.79'N	397.68	9781384.7	188.3	-256.7
Km 4	11° 39.37'N	394.28	9781386.0	181.5	-259.7
Km 5	11° 39.03'N	399.93	9781399.7	214.8	-232.7
Km 6	11° 38.68'N	393.27	9781412.7	209.3	-230.8
Km 7	11° 38.34'N	394.81	9781405.2	208.6	-233.2
Km 8	11° 37.90'N	396.25	9781400.3	220.7	-222.7
Km 9	11° 37.47'N	396.06	9781420.0	232.3	-210.9
Km 10	11° 36.99'N	395.63	9781429.3	243.1	-199.6
Km 11	11° 36.50'N	391.39	9781434.8	238.5	-199.5
Km 12	11° 36.12'N	395.27	9781444.9	262.8	-179.5
Km 13	11° 35.63'N	397.88	9781449.5	278.4	-166.8
Km 14	11° 35.00'N	401.92	9781454.5	299.7	-150.0
Km 15	11° 34.48'N	410.13	9781449.9	323.5	-135.4
Km 16	11° 33.91'N	420.2	9781452.9	361.1	-109.1
Km 17	11° 33.32'N	422.8	9781444.0	363.8	-109.3
Km 18	11° 32.74'N	424.9	9781435.0	364.7	-110.8
Km 19	11° 32.17'N	430.5	9781425.1	375.5	-106.2
Km 20	11° 31.73'N	431.63	9781425.8	382.2	-100.8
Km 21	11° 31.24'N	433.62	9781412.3	377.8	-107.4

.../64

1	2	3	4	5	6
Station Number	Latitude	Height (m)	Absolute Gravity (g.u)	Free Air Anomaly (g.u)	Bouguer Anomaly (g.u)
Km 22	11° 30.81'N	434.1	9781401.9	373.3	-113.1
Km 23	11° 30.34'N	439.03	9781377.0	364.6	-126.7
Km 24	11° 30.00'N	443.15	9781347.7	350.1	-145.8
Km 25	11° 29.89'N	441.63	9781325.5	323.7	-170.5
Km 26	11° 29.45'N	447.36	9781282.0	300.6	-200.0
Km 27	11° 29.08'N	452.35	9781238.5	274.7	-231.5
Km 28	11° 28.73'N	462.70	9781193.7	264.0	-253.8
Km 29	11° 28.45'N	472.28	9781165.5	267.2	-261.3
Km 30	11° 28.04'N	472.43	9781149.6	254.1	-274.5
Km 31	11° 27.62'N	457.08	9781174.3	233.7	-277.8
Km 32	11° 27.25'N	447.93	9781185.4	218.6	-282.6
Km 33	11° 26.79'N	438.87	9781198.3	206.2	-284.9
Km 34	11° 26.52'N	429.83	9781196.2	177.7	-303.3
Km 35	11° 26.14'N	433.34	9781200.5	195.3	-289.7
Km 36	11° 25.76'N	429.06	9781203.6	187.1	-293.0
Km 37	11° 25.19'N	429.59	9781197.8	186.2	-294.5
Km 38	11° 24.66'N	432.10	9781173.8	173.1	-310.4
Km 39	11° 24.57'N	442.43	9781180.6	212.4	-282.7
Km 40	11° 24.69'N	438.93	9781208.4	228.7	-262.5
Km 41	11° 25.11'N	439.02	9781217.5	235.6	-255.7
Km 42	11° 25.52'N	442.89	9781226.9	254.6	-241.0
Km 43	11° 25.60'N	435.36	9781251.3	255.2	-232.0
Km 44	11° 25.68'N	440.37	9781253.1	272.1	-220.7

.../65

1	2	3	4	5	6
Station Number	Latitude	Height (m)	Absolute Gravity (g.u)	Free Air Anomaly (g.u)	Bouguer Anomaly (g.u)
Km 45	11° 25.76'N	441.93	9781262.6	286.0	-208.5
Km 46	11° 24.88'N	432.55	9781254.4	250.7	-233.3
Km 47	11° 24.88'N	432.55	9781244.4	243.8	-240.2
Km 48	11° 24.38'N	448.31	9781246.2	297.3	-204.4
Km 49	11° 23.91'N	453.67	9781257.2	325.7	-182.0
Km 50	11° 23.42'N	448.66	9781264.7	325.6	-176.4
Km 51	11° 22.92'N	448.66	9781264.7	325.6	-176.4
Km 52	11° 22.47'N	444.71	9781287.4	338.6	-159.0
Km 53	11° 21.92'N	451.5	9781277.6	353.0	-152.2
Km 54	11° 21.38'N	441.19	9781316.3	362.9	-130.8
Km 55	11° 20.92'N	447.55	9781329.4	398.4	-102.4
Km 56	11° 20.51'N	444.59	9781343.6	406.3	- 91.7
Km 57	11° 20.11'N	446.23	9781335.1	404.7	- 94.6
Km 58	11° 19.68'N	445.0	9781323.5	391.8	-106.2
Km 59	11° 19.24'N	444.43	9781279.0	348.0	-149.3
Km 60	11° 28.39'N	422.75	9781274.6	223.1	-250.0
Km 61	11° 28.36'N	423.29	9781275.5	225.9	-247.8
Km 62	11° 28.42'N	422.87	9781276.1	224.8	-248.4
Km 63	11° 28.32'N	424.97	9781287.9	243.7	-231.8
Km 64	11° 28.25'N	423.59	9781286.0	237.9	-236.1
Km 65	11° 28.34'N	422.15	9781283.8	230.8	-241.6
Km 66	11° 28.40'N	421.97	9781271.7	217.8	-254.4
Km 67	11° 28.32'N	427.97	9781258.9	224.7	-254.2
Km 68	11° 28.20'N	437.83	9781227.3	225.3	-264.6
Km 69	11° 27.91'N	446.49	9781207.2	234.1	-265.5

.../66

1 Station Number	2 Latitude	3 Height (m)	4 Absolute Gravity (g.u)	5 Free Air Anomaly (g.u)	6 Bouguer Anomaly (g.u)
Km 70	11° 27.57'N	449.08	9781181.6	218.1	-284.4
Km 32	11° 27.25'N	447.93	9781185.4	218.6	-282.6
Km 33	11° 26.79'N	438.87	9781198.3	206.2	-284.9
Km 7	11° 26.66'N	432.99	9781185.9	176.3	-308.2
Km 72	11° 26.39'N	432.3	9781183.5	173.3	-310.4
Km 73	11° 26.11'N	437.86	9781176.0	184.7	-305.3
Km 74	11° 25.65'N	447.00	9781162.1	201.8	-298.4
Km 75	11° 25.22'N	443.49	9781173.3	204.6	-291.7
Km 76	11° 24.78'N	446.8	9781168.7	212.8	-287.2
Km 77	11° 24.30'N	438.87	9781169.5	191.9	-299.2
Km 78	11° 23.83'N	430.37	9781163.1	161.8	-319.8
Km 79	11° 23.75'N	434.19	9781163.5	174.6	-311.3
Km 80	11° 23.70'N	436.8	9781167.5	187.0	-301.8
Km 81	11° 23.64'N	434.2	9781165.2	177.0	-308.9
Km 82	11° 23.53'N	444.01	9781149.3	192.1	-304.7
Km 83	11° 23.43'N	443.28	9781154.7	196.4	-299.6
Km 84	11° 23.33'N	434.86	9781170.9	187.0	-299.6
Km 85	11° 23.24'N	441.54	9781159.9	197.1	-297.0
Km 86	11° 23.16'N	445.59	9781140.3	190.8	-307.8
Km 87	11° 23.05'N	457.87	9781139.0	226.8	-285.6
Km 88	11° 23.16'N	434.07	9781157.8	175.5	-310.2
Km 89	11° 22.54'N	434.66	9781165.4	184.9	-301.5

.../67

1	2	3	4	5	6
Station Number	Latitude	Height (m)	Absolute Gravity (g.u)	Free Air Anomaly (g.u)	Bouguer Anomaly (g.u)
Km 38	11° 24.66'N	432.10	9781173.8	173.1	-310.4
Km 110	11° 24.39'N	432.77	9781172.5	175.7	-308.8
Km 111	11° 24.29'N	428.20	9781177.6	167.0	-312.2
Km 112	11° 24.20'N	426.39	9781192.5	176.8	-300.3
Km 113	11° 24.08'N	422.78	9781186.8	160.6	-312.5
Km 114	11° 23.99'N	425.66	9781168.5	151.7	-324.6
Km 115	11° 23.89'N	430.36	9781160.0	158.4	-323.2
Km 78	11° 23.83'N	430.37	9781163.1	161.8	-319.8
Km 28	11° 28.73'N	462.7	9781193.7	264.0	-253.8
Km 116	11° 28.44'N	471.34	9781173.4	272.2	-255.2
Km 117	11° 28.30'N	474.06	9781173.8	281.9	-248.6
Km 118	11° 28.25'N	479.43	9781122.4	247.3	-289.2
Km 119	11° 27.87'N	485.51	9781115.5	261.6	-281.7
Km 120.	11° 27.32'N	478.2	9781126.2	252.8	-282.3
Km 121	11° 26.78'N	462.10	9781148.4	228.2	-288.9
Km 122	11° 26.25'N	442.96	9781174.4	198.0	-297.7
Km 123	11° 25.79'N	426.92	9781183.2	159.8	-317.9
Km 124	11° 25.25'N	419.52	9781198.6	155.5	-313.9
Km 125	11° 24.95'N	415.46	9781188.1	134.1	-330.8
Km 126	11° 24.39'N	429.02	9781174.5	165.9	-314.2
Km 127	11° 23.75'N	431.92	9781172.1	176.1	-307.2

REFERENCES

Ajakaiye, D.E., 1968. A gravity interpretation of the Ririwai (Liruei) Younger Granite ring complex of N. Nigeria. Geol. Mag. vol. 105, p. 256-263.

.... 1970. Gravity measurements over the Nigerian Younger Granite Province. Nature, vol. 225, p. 50-52.

.... 1974. A gravity profile across the Banke ring complex. Geoexploration, vol. 12, p. 59-66.

.... 1975. Densities of rocks in the Younger Granite Province. Nig. Jol. Mining Geol. vol. 11. p. 33-43.

.... and Burke K., 1972. A Bouguer gravity map of Nigeria. Tectonophysics. vol. 16, p. 108-115.

.... and Sweeney J.F., 1974. Three dimensional gravity interpretation of the Dutsen-Wai complex, Nigerian Younger Granite Province. Tectonophysics, vol. 24; p. 331-341.

.... and Verheijen P.J.T., 1977. Gravity survey across the Quarternary - Basement area of Kano State. Nigerian Society for Mining and Geosciences conference in Zaria.

Amosu, S.N., 1980. Gravity Survey of Dutse Complex in Kano State of Nigeria. Unpublished M.Sc. Thesis Ahmadu Bello University, Zaria.

Bain, A.D.N., 1934. The Younger Intrusive rocks of the Kudaru Hills, Nigeria. Q.J.G.S. vol. XC, p. 201-239.

Bennett, J.N., 1981. The Petrology and mineral chemistry of the Shira complex, Northern Nigeria. Unpubl. Ph.D. Thesis St. Andrews University.

Black, R., 1969. Field occurrences of Niger peralkaline acid rocks. Conference on petrology of peralkaline rocks, University of Reading. Abstracted in Mineral Mag. vol. 37 p. xliii-xliv.

Black, R., and Girod M., 1970. Late Palaeozoic to Recent igneous activity in West Africa and its relationship to Basement structure. In African magmatism and tectonism, Clifford T.N. and Gass I.G. (Eds), Oliver and Boyd, Edinburgh. p. 185-210.

Bott, M.H.P., 1953. Negative Gravity anomalies over Acid "Intrusions" and their Relation to the structure of the Earth's Crust. Geol. Mag., vol. 90, p. 257-267.

.... 1954. Interpretation of the gravity field of the eastern Alps. Geol. Mag. vol. 91, p. 377-383.

.... 1962. A Simple criterion for interpreting negative gravity anomalies. Geophysics, vol. 27, p. 376-381.

.... and Smith R.A., 1958. The estimation of the limiting depth of gravitating bodies. Geophys. Prosp. vol. 6, p. 1-10.

.... and Smithson S.B., 1967. Gravity investigations of subsurface shape and mass distributions of granite batholiths. Geol. Soc. Am. Bull. vol. 78, p. 859-878.

Bowden, P., 1970. Origin of the Younger Granite of Northern Nigeria. Contr. Mineral. Petrol. vol. 25, p. 153-162.

.... and Turner D.C., 1974. Peralkaline and associated ring complexes in the Nigeria - Niger province, West Afric. In The Alkaline Rocks, Sorensen H. (Ed), John Wiley and Sons, 330-351 pp.

Cratchley, C.R., and Jones, G.P., 1965. An Interpretation of the Geology and gravity anomalies of the Benue Valley. Overseas Geol. Surv. Geophysical paper one, p. 1-36.

Clendinning, J. and Olliver, J.G., 1969. Principles and use of surveying instruments, 3rd Ed. : London, Van Nostrand Reinhold Company.

Daly, R.A., 1933. Igneous rocks and the depths of the Earth. Lon. and New York.

Dean, W.C., 1958. Frequency analysis for gravity and magnetic interpretation. Geophysics, vol. 23, p. 281-283.

Dobrin, M.B., 1976. Introduction to Geophysical Prospecting. McGraw-Hill Book Coy. New York.

Du Preez, J.W., 1948. Jos Plateau tin alluvium deposits. Ann. Rep. Geol. Nig. 1947.

Falconer, J.E., 1911. The geology and geography of Northern Nigeria. MacMillan Lon. 295 pp.

Goguel, J. 1950. Interpretation geologigues in measures gravimetrique en Bretague Publ. Bur. Rech. Geol. geophys. vol. 8, p. 30-37.

Grant, F.S. and Elsaharty, A.F., 1962. Bouguer gravity corrections using a variable density. Geophysics, vol. 27, p. 616-626.

.... and West G.F., 1965. Interpretation theory in Applied Geophysics. New York, McGraw-Hill Book Company.

Hansen, D.A., 1966. The search for Iron Ore. Introduction Soc. Expl. Geophys. Mining Geophysics, vol. 1, p. 359-365.

Ike, E.C., 1979. The Petrology and Geochemistry of the Tibchi Younger Granite Ring Complex, N. Nigeria. Unpubl. Ph.D. Thesis. St. Andrews University.

Jacobson, P.R.E., 1947. The Younger Granite complex of the Liruei Hills, Nigeria. Unpubl. Ph.D. Thesis, University of London.

.... Macleod, W.N., and Black, R., 1958. Ring complexes in the Younger Granite Province of Northern Nigeria. Soc. Lond. Proc. No. 1545, p. 21-28.

.... Snelling, N.J. and Truswell, J.F., 1963. Age determination in the geology of Nigeria, with special reference to the Older and Younger Granites. Overseas Geol. and Min. Resources. vol. 9, p. 168-182.

Masson-Smith, D., 1965. Geophysical prospecting for basalt-covered cassiterite on the Jos Plateau, Northern Nigeria. Overseas Geol. Surv. Lond. Geophys. Rep. No. 27.

Nyada, E.N., 1978. The Mafo-D kwa Geophysical Anomalies and their interpretation. Unpubl. Ph.D. Thesis, Ahmadu Bello University, Zaria.

Nagy, D., 1964. The Gravitational effect of two-dimensional masses of arbitrary Cross-section. Pub. Grav. Div. Ottawa.

Nettleton, L.L., 1954. Regional, residuals and structures. Geophysics, vol. 19, p. 1-22.

.... 1971. Elementary Gravity and Magnetics for Geologists and Seismologists. Tulsa Oklahoma S.E.G.

Ojo, S.B., 1974. Gravity investigations in the middle Niger Basin area, Nigeria. Unpubl. M.Sc. Thesis, Ahmadu Bello University, Zaria.

Parasins, D.S., 1976. Principles of Applied Geophysics Lond. Chapman and Hall Ltd.

Roy, A., 1966. Downward Continuation and its application to electromagnetic data interpretation. Geophysics, vol. 4, p. 167-184.

Shaw, S.H., 1950. Report on magnetic and resistivity work in the Plateau Tinfield. Unpubl. Rep. for Geol. Surv. of Nigeria by Overseas Geol. Surv. Lond.

.... and Cole, J.A., 1961. The use of the Electrical Resistivity method for prospecting deep leads in the Jos Plateau Tin-field. Rec. Geol. Surv. Nigeria.

Telford, W.M., Geldart, L.P., Sheriff, R.E. and Keys, D.A., 1979. Applied Geophysics. Cambridge University Press.

Turner, D.C., 1963. Ring Structures in the Sara-Fier Younger Granite complex N. Nigeria, J. Geol. Soc. Lond. vol. 119, p. 345-366.

.... 1968. Review of the Younger Granites of Northern Nigeria. Proceedings of the symposium on the granites of West Africa UNESCO, 1965, 19-21pp.

.... 1972. Structure and tectonic setting of the Younger Granite ring complexes of Nigeria and S. Niger Savanna, vol. 2, p. 51-60.

.... 1976. Structure and petrology of the Younger Granite ring complexes In Geology of Nigeria, Kogbe C.A. (Ed), Elizabethan Publ. Co., Nigeria. 143-158 pp.

.... and Webb P.K., 1974. The Daura igneous complex, N. Nigeria - a Link between the Younger Granite districts of Nigeria and S. Niger. J. Geol. Soc. Lond. vol. 130, p. 71-77.

Vajk, R., 1954. Notes on Frazer S. Grant's paper, A theory for the regional correction of potential field data. Geophysics, vol. 19. p. 569-576.

Van Breemen, O. and Bowden, P., 1973. Sequential age trends for some Nigerian Mesozoic granites. Nature, vol. 242, p. 9-11.

Verheijen, P.J.T., and Ajakaiye, D.E.., 1980. Analysis of errors in barometric elevations in northern Nigeria. Geophysics vol. 45, p. 1144-1152.

Wright, E.P., 1971. The basement complex. Bull. Geol. Surv. Nigeria, vol. 32, p. 12-47.

Wright, J.B., 1972. Parent magmas of Nigeria Younger Granites. Nig. J. Mining and Geol. vol. 7, p. 89-90.